fluctuations, and a significant clinical effect over placebo has been reported (Davidson et al. 2007; Kane et al. 2007; Kramer et al. 2007).

Although the term 'limbic selectivity' has been attributed to second-generation antipsychotics based upon regional differences of dopamine D_2 receptor occupancy between the striatum and extrastriatal regions (Bigliani et al. 2000; Bressan et al. 2003a,b; Grunder et al. 2006; Kessler et al. 2006; Pilowsky et al. 1997; Stephenson et al. 2000; Xiberas et al. 2001), inconsistent results have been reported (Agid et al. 2007; Kessler et al. 2005; Talvik et al. 2001; Yasuno et al. 2001). There are no data in the literature concerning dopamine D_2 receptor occupancy in the striatum and extrastriatal regions by paliperidone.

In this study, we investigated the degree of dopamine D_2 receptor occupancy over a wide dose range of paliperidone ER (3–15 mg) and also compared the striatal and extrastriatal dopamine D_2 receptor occupancy in patients with schizophrenia using positron emission tomography (PET).

Materials and methods

Subjects and study protocol

Thirteen male patients (age range, 22–40 years; mean ± SD, 29.4±5.4 year) diagnosed with schizophrenia, according to the Diagnostic and Statistical Manual of Mental Disorders Fourth Edition criteria, participated in the study (Table 1). This study was conducted as part of an open-label phase II trial of paliperidone ER in Japan (JNS007ER-JPN-S21; Janssen Pharmaceutical K.K.). After complete explanation of the study, written informed consent was obtained from all patients. Exclusion criteria were current or past substance abuse, organic brain disease, epilepsy, or diabetes mellitus. Subjects with severe liver or renal dysfunction, prolonged QTc interval, and treatment with electroconvulsive therapy within 90 days before screening were also excluded. The inclusion criteria were less than 120 of the positive and negative symptom scale (PANSS) score at screening and patients well controlled by only one oral antipsychotic drug during the 4 weeks before the study. Administration of paliperidone ER started on the day after the last administration of the previous drug. The paliperidone ER dose was 3 mg/day in six patients, 9 mg/day in four patients, and 15 mg/day in three patients, given once a day after breakfast for 6 weeks at the same dosage. Clinical symptoms were assessed with PANSS before and 6 weeks after the start of treatment with paliperidone ER. Occurrence of extrapyramidal symptoms (EPS) was assessed by clinical observations without using the standard rating scale. After 2 to 6 weeks, two PET scans per patient were done on the same day, one with [^{11}C]raclopride for striatal dopamine D_2 receptor occupancy and one with [^{11}C]FLB 457 for extrastriatal dopamine D_2 receptor occupancy. The reason for the use of different radioligands was that [^{11}C] raclopride is suitable only for a high-density region such as the striatum, and [^{11}C]FLB 457 is suitable for a low-density extrastriatal region, but its affinity is too high for a high-density region (Ito et al. 1999; Okubo et al. 1999). This

Table 1 Characteristics of the patients, positive and negative symptom scale (PANSS), dopamine D_2 receptor occupancy, plasma concentration of paliperidone ER, and EPS

Patient number	Age (year)	Duration of illness (year)	PANSS		Dose (mg/day)	[^{11}C]raclopride		[^{11}C]FLB 457		EPS
			Before	After		Plasma concentration (ng/ml)	Receptor occupancy (%)	Plasma concentration (ng/ml)	Receptor occupancy (%)	
1	28	7.9	59	55	3	7.04	54.2	7.44	58.9	−
2	21	2.2	36	34	3	7.78	58.4	7.5	34.5	−
3	28	5.5	49	46	3	6.32	55.1	6.62	53.3	−
4	35	13	68	67	3	8.33	66.7	8.84	63.0	−
5	22	0.2	77	73	3	12.8	56.2	12.3	37.5	−
6	28	8.1	70	61	3	9.9	56.8	10.2	71.1	−
7	22	7.9	99	96	9	21.4	71.4	20.6	78.7	−
8	33	7.9	60	56	9	57	81.8	51.9	64.6	−
9	25	7.8	43	42	9	27.1	72.1	23.2	74.1	−
10	39	5.4	79	71	9	59.9	84.3	65.2	87.3	+
11	28	0.2	55	38	15	48.2	85.5	43.6	79.6	+
12	33	12.3	65	65	15	14.5	73.7	13.4	74.3	+
13	31	6.9	58	56	15	54.2	82.1	51.7	79.1	−
mean	29	6.6	62.9	58.5						
SD	5.4	3.9	16.5	16.8						

study was approved by the Ethics and Radiation Safety Committee of the National Institute of Radiological Sciences, Chiba, Japan.

PET procedure

A PET scanner system, ECAT EXACT HR + (CTI-Siemens, Knoxville, TN, USA), was used to measure regional brain radioactivity. To minimize head movement, a head fixation device (Fixter, Stockholm, Sweden) was used. A transmission scan for attenuation correction was performed using a ^{68}Ge-^{68}Ga source before each scan. Dynamic PET scanning was performed for 60 min after intravenous bolus injection of 214.3–260.0 MBq of [^{11}C]raclopride. The specific radioactivity of [^{11}C]raclopride was 118.7–294.2 GBq/μmol (mean ± SD, 201.9±45.2 GBq/μmol). One hour after the end of the [^{11}C]raclopride PET measurement, dynamic PET scanning was performed for 80 min after intravenous bolus injection of 218.0–237.4 MBq of [^{11}C]FLB 457. The specific radioactivity of [^{11}C]FLB 457 was 104.7–418.6 GBq/μmol (mean ± SD, 299.3±112.2 GBq/μmol). Magnetic resonance (MR) images of the brain were acquired with 1.5 T MR imaging, Gyroscan NT (Philips Medical Systems, Best, The Netherlands). T_1-weighted MR images at 1-mm slices were obtained. Venous blood samples were obtained immediately before tracer injection for each PET scan to measure the plasma concentration of paliperidone.

Data analysis

All emission scans were reconstructed with a Hanning filter cut-off frequency of 0.4. Regions of interest (ROIs) were defined for the striatum ([^{11}C]raclopride), temporal cortex ([^{11}C]FLB 457), and cerebellum ([^{11}C]raclopride and [^{11}C] FLB 457). The ROIs were drawn manually on the summated PET images with reference to the individual MR images. The average values of right and left ROIs were used for the analysis. Dopamine D_2 receptor binding was quantified using a three-parameter simplified reference tissue model (Ito et al. 2001; Lammertsma and Hume 1996). The cerebellum was used as the reference tissue given its negligible density of dopamine D_2 receptors (Suhara et al. 1999). This model allows the estimation of binding potential (BP_{ND}), which was defined as $f_{ND} \times B_{max}/K_d$, where f_{ND} is the free fraction of ligand in the nondisplaceable tissue compartment, B_{max} is the receptor density, and K_d is the dissociation constant (Innis et al. 2007).

The dopamine D_2 receptor occupancy by paliperidone was estimated using the following equation: occupancy(%) = $(BP_{base} - BP_{drug})/BP_{base} \times 100$, where BP_{base} is the BP_{ND} in the drug-free state, and BP_{drug} is the BP_{ND} after administration of paliperidone (Takano et al. 2004; Takano et al. 2006a, b; Yasuno et al. 2001). In this study, the mean BP_{ND} in age-matched normal male subjects (n=13; age range 22–40 years; mean ± SD, 29.2±5.5 years) was used as BP_{base}, as BP_{ND} in the striatum measured with [^{11}C]raclopride or in the temporal cortex measured with [^{11}C]FLB 457 in patients with schizophrenia is not significantly different from that in the normal control (Farde et al. 1990; Suhara et al. 2002; Talvik et al. 2003). The PET procedure and data analysis for the BP_{ND} estimation of normal subjects were the same as those for the patients. The relationship between the dose or plasma concentration of paliperidone and dopamine D_2 receptor occupancy is described by the following equation: occupancy(%) = $C/(C + ED_{50}) \times 100$, where C is the dose or plasma concentration of paliperidone, and ED_{50} is the dose or plasma concentration required to induce 50% occupancy (Nyberg et al. 1999; Takano et al. 2004; Takano et al. 2006a, b; Yasuno et al. 2001). In this study, maximum occupancy was fixed at 100%, the same as previous occupancy studies of risperidone (Nyberg et al. 1999; Yasuno et al. 2001).

Measurement of plasma concentration of paliperidone

Blood samples were collected in heparinized tubes and centrifuged for 10 min at 3,000 rpm. Separated plasma samples were stored at −20°C. Plasma concentrations of paliperidone were determined using a validated liquid chromatography coupled to mass spectrometry/mass spectrometry (LC–MS/MS) method with a target lower limit of quantification of 0.10 ng/ml (Johnson & Johnson Pharmaceutical Research and Development L. L. C., Beerse, Belgium).

Statistical analysis

Correlations between dose or plasma concentration of paliperidone and dopamine D_2 receptor occupancy in the striatum and temporal cortex were assessed. Correlations between striatal occupancy and age or duration of illness were also assessed. Paired t tests were performed to compare (1) dopamine D_2 receptor occupancies between the striatum and temporal cortex and (2) plasma concentrations of paliperidone between the two PET scans, with [^{11}C]raclopride and [^{11}C]FLB 457, in each individual subject. In all tests, a p value<0.05 was considered statistically significant.

Results

The dopamine D_2 receptor occupancy in the striatum measured with [^{11}C]raclopride was 54.2 to 85.5% (Table 1). Mean dopamine D_2 receptor occupancies in the striatum were 57.9±4.5% at 3 mg/day, 77.4±6.6% at 9 mg/day, and 80.4±6.1% at 15 mg/day. ED_{50} in the striatum was 2.38 mg/day (r=0.86) and 6.65 ng/ml (r=0.82; Fig. 1).

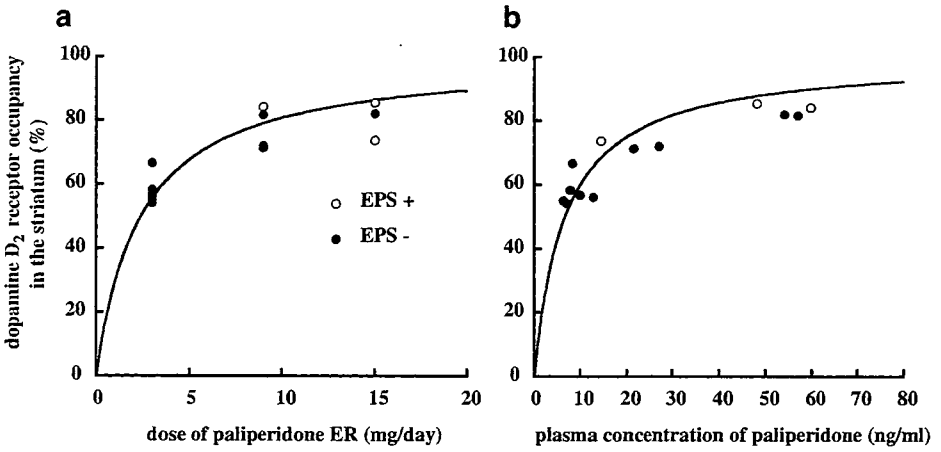

Fig. 1 Relationship between dopamine D_2 receptor occupancy in the striatum and dose (**a**) or plasma concentration (**b**) of paliperidone ER in the [^{11}C] raclopride study. ED_{50} in the striatum was 2.38 mg/day (r=0.86) and 6.65 ng/ml (r=0.82)

The dopamine D_2 receptor occupancy in the temporal cortex measured with [^{11}C]FLB 457 was 34.5 to 87.3%. Mean dopamine D_2 receptor occupancies were 53.1±14.5% at 3 mg/day, 76.2±9.5% at 9 mg/day, and 77.7±3.0% at 15 mg/day in the temporal cortex. ED_{50} in the temporal cortex was 2.84 mg/day (r=0.73) and 7.73 ng/ml (r=0.61; Fig. 2). There were no significant differences in plasma concentrations of paliperidone between the two scans (p= 0.24) and in dopamine D_2 receptor occupancy between the striatum and temporal cortex at any dose (p=0.30).

There were no correlations between striatal occupancy and age (p=0.07) or duration of illness (p=0.90).

Average PANSS scores of all patients were 62.9±16.5 before taking paliperidone ER and 58.5±16.8 after 6 weeks. Three patients, two taking 15 mg and one 9 mg (no. 10, 11, 12), showed EPS (Table 1).

Discussion

The present study demonstrated that the ED_{50} of striatal dopamine D_2 receptor occupancy of paliperidone ER was 2.38 mg/day and that of the temporal cortex was 2.84 mg/day. Previous studies reported that the striatal ED_{50} of risperidone was 1.2 mg/day (Nyberg et al. 1999) and that the limbic-cortical ED_{50} was 1.46 mg/day (Yasuno et al. 2001). These studies indicate that the equivalent ratio for a daily dose between risperidone and paliperidone ER seems to be about 1:2. The striatal and temporal ED_{50} values of plasma concentration of paliperidone were 6.65 and 7.73 ng/ml, respectively, almost matching the values previously reported for risperidone active moiety (6.87 ng/ml, Nyberg et al. 1999; 7.43 ng/ml, Yasuno et al. 2001) for striatal and limbic–cortical regions, respectively. The therapeutic dose ranges of paliperidone ER calculated from ED_{50} were 5.6–9.5 mg/day and 15.5–26.6 ng/ml. In two previous studies (Nyberg et al. 1999; Yasuno et al. 2001), the sum of risperidone and paliperidone was regarded as risperidone active moiety. Because paliperidone shows almost the same affinity for dopamine D_2 receptor as risperidone, the effect for dopamine D_2 receptor was about the same between risperidone active moiety and paliperidone. This suggests that similar dopamine D_2 receptor occupancy is achieved with comparable plasma concen-

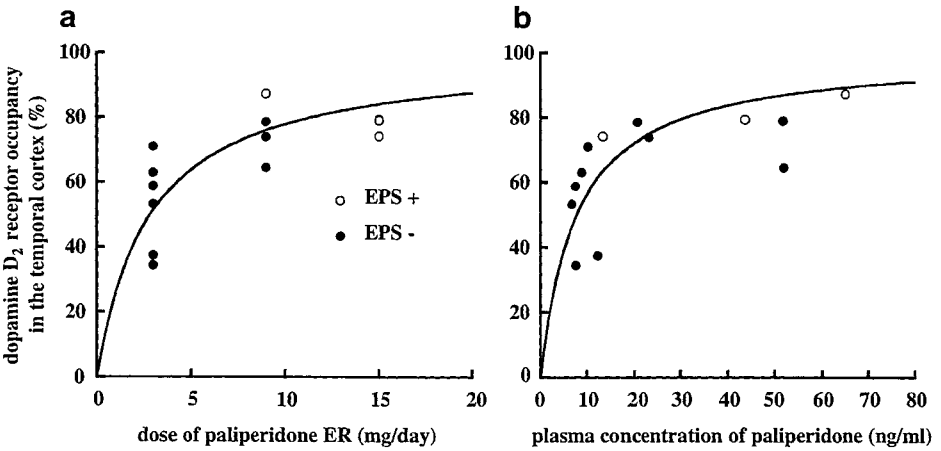

Fig. 2 Relationship between dopamine D_2 receptor occupancy in the temporal cortex and dose (**a**) or plasma concentration (**b**) of paliperidone ER in the [^{11}C]FLB 457 study. ED_{50} in the temporal cortex was 2.84 mg/day (r=0.73) and 7.73 ng/ml (r=0.61)

trations of paliperidone or risperidone active moiety. This finding confirms that paliperidone is as effective in crossing the blood–brain barrier as the active moiety of risperidone.

In the previous PET study that administered a single dose of paliperidone ER at 6 mg to four healthy Caucasian subjects, the striatal dopamine D_2 receptor occupancy fluctuation derived was 75–78%, and ED_{50} was 4.4 ng/ml (Karlsson et al., presented at WWS 2006). The differences between the two studies may be explained by the small number of observations and/or ethnicity. In the present study, occupancy was measured at steady-state drug levels (after multiple doses), whereas the previous study was carried out after a single dose.

There were no significant differences between striatal and extrastriatal dopamine D_2 receptor occupancy by paliperidone. Although the interval between the two scans was 2 h, the difference in plasma concentrations of paliperidone between them was about 7%, statistically not different as paliperidone ER tablets were made for flat plasma concentrations at a steady state. There have been discussions about the concept of 'limbic selectivity,' i.e., low dopamine D_2 receptor occupancy in the striatum and high occupancy in the extrastriatum (Pilowsky et al. 1997). It was reported in some second-generation antipsychotics such as clozapine (Grunder et al. 2006; Kessler et al. 2006; Pilowsky et al. 1997; Xiberas et al. 2001), olanzapine (Bigliani et al. 2000; Xiberas et al. 2001), amisulpiride (Bressan et al. 2003a; Xiberas et al. 2001), and quetiapine (Kessler et al. 2006; Stephenson et al. 2000) using [^{123}I] epidepride, [^{76}Br]FLB 457 or [^{18}F]fallypride. However, no significant difference between the striatum and extrastriatal regions have been reported using two different ligands, [^{11}C]raclopride and [^{11}C]FLB 457 (Agid et al. 2007; Talvik et al. 2001), or one ligand, [^{18}F]fallypride (Kessler et al. 2005). Human dopamine D_2 receptor occupancy by risperidone also showed inconsistent results. Two studies showed higher occupancy in the temporal cortex than in the striatum using [^{123}I]epidepride (75% in the temporal cortex and 50% in the striatum; Bressan et al. 2003b) and [^{76}Br] FLB 457 (91.6% in the temporal cortex and 63.3% in the striatum; Xiberas et al. 2001). On the other hand, similar occupancy values by risperidone were reported in the striatum (53–85%) using [^{11}C]raclopride (Nyberg et al. 1999) and extrastriatal regions (38–80%) using [^{11}C]FLB 457 (Yasuno et al. 2001). Because several factors such as scanning time, ligand selection, kinetic modeling, etc. need to be considered (Erlandsson et al. 2003; Olsson and Farde 2001), we used two different ligands to measure the different receptor density regions with appropriate scanning time and kinetic modeling for each ligand (Olsson and Farde 2001). Our results indicated no significant difference in regional occupancy (Agid et al. 2007; Kessler et al. 2005; Talvik et al. 2001; Yasuno et al. 2001). Although extrastriatal regions are suggested to be sites for antipsychotic action (Lidow et al. 1998), a recent study reported that extrastriatal dopamine D_2 receptor occupancy did not correlate with the antipsychotic effect (Agid et al. 2007).

In the present study, three patients complained of EPS. Average striatal occupancy of these three patients was 80.8%, a level in line with that known to increase the likelihood for EPS (Farde et al. 1992; Kapur et al. 2000; Nordstrom et al. 1993).

Previous studies indicated that over 70% of dopamine D_2 receptor occupancy is required for antipsychotic effects in patients with schizophrenia in the acute phase (Kapur et al. 2000; Nordstrom et al. 1993). In chronic treatment, haloperidol decanoate showed 73% occupancy at 1 week after injection and 52% occupancy at 4 weeks (Nyberg et al. 1995). Long-acting injectable risperidone showed 25–83 or 53–79% occupancy at a steady state (Gefvert et al. 2005; Remington et al. 2006). It is difficult to link the degree of dopamine D_2 receptor occupancy to a clinical effect, as almost all our patients (except nos. 5 and 11) had been undergoing long-term treatment when they entered the study. However, in all patients, these scores decreased with treatment or remained stable (Table 1) irrespective of dose. Furthermore, in all patients, striatal dopamine D_2 receptor occupancies above 50% were noted. This indicates that, for maintenance therapy of patients with schizophrenia, over 70% dopamine D_2 receptor occupancy might not necessarily be required. However, as this was an open-label study, further studies (such as randomized controlled trials) would be needed for an exact estimation of the threshold of dopamine D_2 receptor occupancy in the treatment of chronic patients with schizophrenia.

The half-life of paliperidone is about 28 h (data on file). High receptor occupancy is sustained when the plasma half-life of the treatment is long (Takano et al. 2004). Sustained high dopamine D_2 receptor occupancy can be expected at dosages of 9 or 15 mg/day of paliperidone ER. As EPS are a frequent reason for interruption of drug treatment (Lieberman et al. 2005), although the therapeutic dose range of paliperidone ER calculated from ED_{50} was 5.6–9.5 mg/day, for chronic treatment, lower doses might be useful, avoiding dopamine D_2 receptor occupancy rates above 80%. The estimated dopamine D_2 receptor occupancy at 6 mg/day of paliperidone ER was about 72%, in a range associated with efficacy (dopamine D_2 receptor occupancy above 70%) but not above a level associated with increased risks of extrapyramidal side effects (dopamine D_2 receptor occupancy above 80%).

To calculate the dopamine D_2 receptor occupancy in this study, we used BP_{ND} of normal control subjects as a surrogate for BP_{ND} in the drug-free state. Although previous studies showed no difference in dopamine D_2 receptor density in the striatum (Farde et al. 1990) or in the

temporal cortex (Suhara et al. 2002; Talvik et al. 2003) between the normal subjects and the patients with schizophrenia, individual differences in dopamine D_2 receptor density might potentially lead to an error in the estimation of dopamine D_2 receptor occupancy (Farde et al. 1992). For example, if BP_{base} changes from −13% to +15%, the range of the present study, the calculated 50% occupancy could be changed from 43 to 57%. The effect of a small portion of displaceable binding in the cerebellum (Delforge et al. 2001; Hall et al. 1996) may lead to an underestimation from 50% of [^{11}C]FLB 457 occupancy to 46% (Olsson et al. 2004). These factors may explain the differences in dopamine D_2 receptor occupancy between the striatum and temporal cortex in some patients.

Conclusions

The data from this study suggest that paliperidone ER at 6–9 mg provides an estimated level of dopamine D_2 receptor occupancy between 70–80%. The magnitude of dopamine D_2 receptor occupancy is similar between the striatum and temporal cortex.

Acknowledgment This study was supported by Janssen Pharmaceutical K.K. and the National Institute of Radiological Sciences. We extend our thanks to Dr. Shoko Nozaki, Dr. Amane Tateno, Dr. Tetsuya Ichimiya, Dr. Koichiro Watanabe, Dr. Kensuke Nomura, Dr. Takashi Nakayama, Mr. Katsuyuki Tanimoto, Mr. Takahiro Shiraishi, Mr. Akira Ando, and Ms. Yoshiko Fukushima for their help with this study.

References

Agid O, Mamo D, Ginovart N, Vitcu I, Wilson AA, Zipursky RB, Kapur S (2007) Striatal vs extrastriatal dopamine D2 receptors in antipsychotic response—a double-blind PET study in schizophrenia. Neuropsychopharmacology 32:1209–1215

Bigliani V, Mulligan RS, Acton PD, Ohlsen RI, Pike VW, Ell PJ, Gacinovic S, Kerwin RW, Pilowsky LS (2000) Striatal and temporal cortical D2/D3 receptor occupancy by olanzapine and sertindole in vivo: a [123I]epidepride single photon emission tomography (SPET) study. Psychopharmacology (Berl) 150:132–140

Bressan RA, Erlandsson K, Jones HM, Mulligan R, Flanagan RJ, Ell PJ, Pilowsky LS (2003a) Is regionally selective D2/D3 dopamine occupancy sufficient for atypical antipsychotic effect? An in vivo quantitative [123I]epidepride SPET study of amisulpride-treated patients. Am J Psychiatry 160:1413–1420

Bressan RA, Erlandsson K, Jones HM, Mulligan RS, Ell PJ, Pilowsky LS (2003b) Optimizing limbic selective D2/D3 receptor occupancy by risperidone: a [123I]-epidepride SPET study. J Clin Psychopharmacol 23:5–14

Davidson M, Emsley R, Kramer M, Ford L, Pan G, Lim P, Eerdekens M (2007) Efficacy, safety and early response of paliperidone extended-release tablets (paliperidone ER): Results of a 6-week, randomized, placebo-controlled study. Schizophr Res 93:117–130

Delforge J, Bottlaender M, Loc'h C, Dolle F, Syrota A (2001) Parametric images of the extrastriatal D2 receptor density obtained using a high-affinity ligand (FLB 457) and a double-saturation method. J Cereb Blood Flow Metab 21:1493–1503

Erlandsson K, Bressan RA, Mulligan RS, Ell PJ, Cunningham VJ, Pilowsky LS (2003) Analysis of D2 dopamine receptor occupancy with quantitative SPET using the high-affinity ligand [123I]epidepride: resolving conflicting findings. Neuroimage 19:1205–1214

Farde L, Wiesel FA, Stone-Elander S, Halldin C, Nordstrom AL, Hall H, Sedvall G (1990) D2 dopamine receptors in neuroleptic-naive schizophrenic patients. A positron emission tomography study with [11C]raclopride. Arch Gen Psychiatry 47:213–219

Farde L, Nordstrom AL, Wiesel FA, Pauli S, Halldin C, Sedvall G (1992) Positron emission tomographic analysis of central D1 and D2 dopamine receptor occupancy in patients treated with classical neuroleptics and clozapine. Relation to extrapyramidal side effects. Arch Gen Psychiatry 49:538–544

Gefvert O, Eriksson B, Persson P, Helldin L, Bjorner A, Mannaert E, Remmerie B, Eerdekens M, Nyberg S (2005) Pharmacokinetics and D2 receptor occupancy of long-acting injectable risperidone (Risperdal Consta) in patients with schizophrenia. Int J Neuropsychopharmacol 8:27–36

Grunder G, Landvogt C, Vernaleken I, Buchholz HG, Ondracek J, Siessmeier T, Hartter S, Schreckenberger M, Stoeter P, Hiemke C, Rosch F, Wong DF, Bartenstein P (2006) The striatal and extrastriatal D2/D3 receptor-binding profile of clozapine in patients with schizophrenia. Neuropsychopharmacology 31:1027–1035

Hall H, Farde L, Halldin C, Hurd YL, Pauli S, Sedvall G (1996) Autoradiographic localization of extrastriatal D2-dopamine receptors in the human brain using [125I]epidepride. Synapse 23:115–123

Innis RB, Cunningham VJ, Delforge J, Fujita M, Gjedde A, Gunn RN, Holden J, Houle S, Huang SC, Ichise M, Iida H, Ito H, Kimura Y, Koeppe RA, Knudsen GM, Knuuti J, Lammertsma AA, Laruelle M, Logan J, Maguire RP, Mintun MA, Morris ED, Parsey R, Price JC, Slifstein M, Sossi V, Suhara T, Votaw JR, Wong DF, Carson RE (2007) Consensus nomenclature for in vivo imaging of reversibly binding radioligands. J Cereb Blood Flow Metab 27:1533–1539

Ito H, Okubo Y, Halldin C, Farde L (1999) Mapping of central D2 dopamine receptors in man using [11C]raclopride: PET with anatomic standardization technique. Neuroimage 9:235–242

Ito H, Sudo Y, Suhara T, Okubo Y, Halldin C, Farde L (2001) Error analysis for quantification of [11C]FLB 457 binding to extrastriatal D2 dopamine receptors in the human brain. Neuroimage 13:531–539

Kane J, Canas F, Kramer M, Ford L, Gassmann-Mayer C, Lim P, Eerdekens M (2007) Treatment of schizophrenia with paliperidone extended-release tablets: a 6-week placebo-controlled trial. Schizophr Res 90:147–161

Kapur S, Zipursky R, Jones C, Remington G, Houle S (2000) Relationship between dopamine D2 occupancy, clinical response, and side effects: a double-blind PET study of first-episode schizophrenia. Am J Psychiatry 157:514–520

Kessler RM, Ansari MS, Riccardi P, Li R, Jayathilake K, Dawant B, Meltzer HY (2005) Occupancy of striatal and extrastriatal dopamine D2/D3 receptors by olanzapine and haloperidol. Neuropsychopharmacology 30:2283–2289

Kessler RM, Ansari MS, Riccardi P, Li R, Jayathilake K, Dawant B, Meltzer HY (2006) Occupancy of striatal and extrastriatal dopamine D2 receptors by clozapine and quetiapine. Neuropsychopharmacology 31:1991–2001

Kramer M, Simpson G, Maciulis V, Kushner S, Vijapurkar U, Lim P, Eerdekens M (2007) Paliperidone extended-release tablets for prevention of symptom recurrence in patients with schizophrenia: a randomized, double-blind, placebo-controlled study. J Clin Psychopharmacol 27:6–14

Lammertsma AA, Hume SP (1996) Simplified reference tissue model for PET receptor studies. Neuroimage 4:153–158

Leysen JE, Gommeren W, Eens A, de Chaffoy de Courcelles D, Stoof JC, Janssen PA (1988) Biochemical profile of risperidone, a new antipsychotic. J Pharmacol Exp Ther 247:661–670

Leysen JE, Janssen PM, Megens AA, Schotte A (1994) Risperidone: a novel antipsychotic with balanced serotonin–dopamine antagonism, receptor occupancy profile, and pharmacologic activity. J Clin Psychiatry 55(Suppl):5–12

Lidow MS, Williams GV, Goldman-Rakic PS (1998) The cerebral cortex: a case for a common site of action of antipsychotics. Trends Pharmacol Sci 19:136–140

Lieberman JA, Stroup TS, McEvoy JP, Swartz MS, Rosenheck RA, Perkins DO, Keefe RS, Davis SM, Davis CE, Lebowitz BD, Severe J, Hsiao JK (2005) Effectiveness of antipsychotic drugs in patients with chronic schizophrenia. N Engl J Med 353:1209–1223

Nordstrom AL, Farde L, Wiesel FA, Forslund K, Pauli S, Halldin C, Uppfeldt G (1993) Central D2-dopamine receptor occupancy in relation to antipsychotic drug effects: a double-blind PET study of schizophrenic patients. Biol Psychiatry 33:227–235

Nyberg S, Farde L, Halldin C, Dahl ML, Bertilsson L (1995) D2 dopamine receptor occupancy during low-dose treatment with haloperidol decanoate. Am J Psychiatry 152:173–178

Nyberg S, Eriksson B, Oxenstierna G, Halldin C, Farde L (1999) Suggested minimal effective dose of risperidone based on PET-measured D2 and 5-HT2A receptor occupancy in schizophrenic patients. Am J Psychiatry 156:869–875

Okubo Y, Olsson H, Ito H, Lofti M, Suhara T, Halldin C, Farde L (1999) PET mapping of extrastriatal D2-like dopamine receptors in the human brain using an anatomic standardization technique and [11C]FLB 457. Neuroimage 10:666–674

Olsson H, Farde L (2001) Potentials and pitfalls using high affinity radioligands in PET and SPET determinations on regional drug induced D2 receptor occupancy—a simulation study based on experimental data. Neuroimage 14:936–945

Olsson H, Halldin C, Farde L (2004) Differentiation of extrastriatal dopamine D2 receptor density and affinity in the human brain using PET. Neuroimage 22:794–803

Pilowsky LS, Mulligan RS, Acton PD, Ell PJ, Costa DC, Kerwin RW (1997) Limbic selectivity of clozapine. Lancet 350:490–491

Remington G, Mamo D, Labelle A, Reiss J, Shammi C, Mannaert E, Mann S, Kapur S (2006) A PET study evaluating dopamine D2 receptor occupancy for long-acting injectable risperidone. Am J Psychiatry 163:396–401

Stephenson CM, Bigliani V, Jones HM, Mulligan RS, Acton PD, Visvikis D, Ell PJ, Kerwin RW, Piłowsky LS (2000) Striatal and extra-striatal D2/D3 dopamine receptor occupancy by quetiapine in vivo. [123I]-epidepride single photon emission tomography (SPET) study. Br J Psychiatry 177:408–415

Suhara T, Sudo Y, Okauchi T, Maeda J, Kawabe K, Suzuki K, Okubo Y, Nakashima Y, Ito H, Tanada S, Halldin C, Farde L (1999) Extrastriatal dopamine D2 receptor density and affinity in the human brain measured by 3D PET. Int J Neuropsychopharmcol 2:73–82

Suhara T, Okubo Y, Yasuno F, Sudo Y, Inoue M, Ichimiya T, Nakashima Y, Nakayama K, Tanada S, Suzuki K, Halldin C, Farde L (2002) Decreased dopamine D2 receptor binding in the anterior cingulate cortex in schizophrenia. Arch Gen Psychiatry 59:25–30

Takano A, Suhara T, Ikoma Y, Yasuno F, Maeda J, Ichimiya T, Sudo Y, Inoue M, Okubo Y (2004) Estimation of the time-course of dopamine D2 receptor occupancy in living human brain from plasma pharmacokinetics of antipsychotics. Int J Neuropsychopharmacol 7:19–26

Takano A, Suhara T, Kusumi I, Takahashi Y, Asai Y, Yasuno F, Ichimiya T, Inoue M, Sudo Y, Koyama T (2006a) Time course of dopamine D2 receptor occupancy by clozapine with medium and high plasma concentrations. Prog Neuropsychopharmacol Biol Psychiatry 30:75–81

Takano A, Suhara T, Yasuno F, Suzuki K, Takahashi H, Morimoto T, Lee YJ, Kusuhara H, Sugiyama Y, Okubo Y (2006b) The antipsychotic sultopride is overdosed—a PET study of drug-induced receptor occupancy in comparison with sulpiride. Int J Neuropsychopharmacol 9:539–545

Talvik M, Nordstrom AL, Nyberg S, Olsson H, Halldin C, Farde L (2001) No support for regional selectivity in clozapine-treated patients: a PET study with [11C]raclopride and [11C]FLB 457. Am J Psychiatry 158:926–930

Talvik M, Nordstrom AL, Olsson H, Halldin C, Farde L (2003) Decreased thalamic D2/D3 receptor binding in drug-naive patients with schizophrenia: a PET study with [11C]FLB 457. Int J Neuropsychopharmacol 6:361–370

Xiberas X, Martinot JL, Mallet L, Artiges E, Loc HC, Maziere B, Paillere-Martinot ML (2001) Extrastriatal and striatal D2 dopamine receptor blockade with haloperidol or new antipsychotic drugs in patients with schizophrenia. Br J Psychiatry 179:503–508

Yasuno F, Suhara T, Okubo Y, Sudo Y, Inoue M, Ichimiya T, Tanada S (2001) Dose relationship of limbic-cortical D2-dopamine receptor occupancy with risperidone. Psychopharmacology (Berl) 154:112–114

ELSEVIER

NeuroImage

www.elsevier.com/locate/ynimg
NeuroImage 39 (2008) 555–565

Normal database of dopaminergic neurotransmission system in human brain measured by positron emission tomography

Hiroshi Ito,* Hidehiko Takahashi, Ryosuke Arakawa, Harumasa Takano, and Tetsuya Suhara

Clinical Neuroimaging Team, Molecular Neuroimaging Group, Molecular Imaging Center, National Institute of Radiological Sciences, 4-9-1 Anagawa, Inage-ku, Chiba 263-8555, Japan

Received 19 April 2007; revised 31 August 2007; accepted 7 September 2007
Available online 19 September 2007

The central dopaminergic system is of interest in the pathophysiology of schizophrenia and other neuropsychiatric disorders. Both pre- and postsynaptic dopaminergic functions can be estimated by positron emission tomography (PET) with different radiotracers. However, an integrated database of both pre- and postsynaptic dopaminergic neurotransmission components including receptors, transporter, and endogenous neurotransmitter synthesis has not yet been reported. In the present study, we constructed a normal database for the pre- and postsynaptic dopaminergic functions in the living human brain using PET. To measure striatal and extrastriatal dopamine D_1 and D_2 receptor bindings, dopamine transporter binding, and endogenous dopamine synthesis rate, PET scans were performed on healthy men after intravenous injection of [^{11}C]SCH23390, [^{11}C]raclopride, [^{11}C]FLB457, [^{11}C]PE2I, or L-[β-^{11}C]DOPA. All PET images were anatomically standardized using SPM2, and a database was built for each radiotracer. Gray matter images were segmented and extracted from all anatomically standardized magnetic resonance images using SPM2, and they were used for partial volume correction. These databases allow the comparison of regional distributions of striatal and extrastriatal dopamine D_1 and D_2 receptors, dopamine transporter, and endogenous dopamine synthesis capability. These distributions were in good agreement with those from human postmortem studies. This database can be used in various researches to understand the physiology of dopaminergic functions in the living human brain. This database could also be used to investigate regional abnormalities of dopaminergic neurotransmission in neuropsychiatric disorders.

Introduction

The central dopaminergic system is of major interest in the pathophysiology of schizophrenia and other neuropsychiatric disorders. Both pre- and postsynaptic dopaminergic functions can be estimated by positron emission tomography (PET) and single-photon emission computed tomography (SPECT) with the use of several radiotracers. The binding of dopamine receptors representing postsynaptic functions can be measured for each of D_1 and D_2 subtypes. For measurement of dopamine D_1 receptor binding, [^{11}C]SCH23390 (Farde et al., 1987a; Halldin et al., 1986) and [^{11}C]NNC112 (Halldin et al., 1998) are widely used. To measure the binding of striatal and extrastriatal dopamine D_2 receptors, which are quite different in densities, [^{11}C]raclopride (Farde et al., 1985; Ito et al., 1998; Kohler et al., 1985) and [^{11}C]FLB457 (Halldin et al., 1995; Ito et al., 2001; Suhara et al., 1999), respectively, are widely used. The bindings of striatal (Farde et al., 1987b, 1990; Nordstrom et al., 1995) and extrastriatal (Suhara et al., 2002; Yasuno et al., 2004) dopamine D_2 receptors in schizophrenia have been investigated. For estimation of the presynaptic dopaminergic function, dopamine transporter binding is measured by [^{11}C]β-CIT (Farde et al., 1994; Muller et al., 1993), [^{11}C]PE2I (Emond et al., 1997; Hall et al., 1999), and other radioligands. The endogenous dopamine synthesis rate measured by 6-[^{18}F]fluoro-L-DOPA (Gjedde, 1988; Gjedde et al., 1991; Huang et al., 1991) and L-[β-^{11}C]DOPA (Hartvig et al., 1991; Tedroff et al., 1992) can also indicate the presynaptic dopaminergic function. Dopamine transporter binding (Laakso et al., 2000; Laruelle et al., 2000) and the endogenous dopamine synthesis rate (Hietala et al., 1995; Laruelle, 1998; Lindstrom et al., 1999; Reith et al., 1994) in schizophrenia have been investigated.

An anatomic standardization technique, consisting of the transformation of brain images of individual subjects into a standard brain shape and size in three dimensions, allows inter-subject averaging of PET images (Fox et al., 1988; Friston et al., 1990). Using this technique with calculation of PET parametric images, a database of the regional distribution of neurotransmission functions can be constructed, and from this, group comparisons between normal control subjects and patients on a voxel-by-voxel basis can be performed. Previously, we built a normal database for the striatal and extrastriatal dopamine D_2 receptor bindings representing the postsynaptic dopaminergic neurotransmission components in the living human brain (Ito et al., 1999; Okubo et al., 1999). The in vivo regional distribution of dopamine D_2 receptor binding was in good agreement with that known from in vitro studies. For presynaptic dopaminergic function, a normal database for the endogenous dopamine synthesis rate in the living human brain has also been constructed with the use of 6-[^{18}F]fluoro-L-DOPA (Nagano et al.,

* Corresponding author. Fax: +81 43 253 0396.
E-mail address: hito@nirs.go.jp (H. Ito).
Available online on ScienceDirect (www.sciencedirect.com).

1053-8119/$ - see front matter © 2007 Elsevier Inc. All rights reserved.
doi:10.1016/j.neuroimage.2007.09.011

2000). However, an integrated database for both pre- and postsynaptic dopaminergic neurotransmission components including receptors, transporter, and endogenous neurotransmitter synthesis, which allows to compare regional distributions between neurotransmission components on a same coordinate, has not been reported. In the present study, we constructed a normal database for pre- and postsynaptic dopaminergic neurotransmission components in the living human brain using PET and the anatomic standardization technique. Striatal and extrastriatal dopamine D_1 and D_2 receptor bindings, dopamine transporter binding, and endogenous dopamine synthesis rate were measured in healthy volunteers using the radiotracers [^{11}C]SCH23390, [^{11}C]raclopride, [^{11}C]FLB457, [^{11}C]PE2I, and L-[β-^{11}C]DOPA.

Materials and methods

Subjects

The study was approved by the Ethics and Radiation Safety Committees of the National Institute of Radiological Sciences, Chiba, Japan. A total of 37 healthy men were recruited, and they gave their written informed consent for participation in the study (Table 1). The subjects were free of somatic, neurological or psychiatric disorders on the basis of their medical history and magnetic resonance (MR) imaging of the brain. They had no history of current or previous drug abuse and had not taken dopaminergic drugs in the past two weeks. Both PET studies with [^{11}C]raclopride and [^{11}C]FLB457 were performed in the same subjects on the same day. For [^{11}C]SCH23390, [^{11}C]PE2I, and L-[β-^{11}C]DOPA studies, each subject underwent only one PET study except three subjects: two underwent L-[β-^{11}C]DOPA, [^{11}C]raclopride, and [^{11}C]FLB457 studies; one underwent L-[β-^{11}C]DOPA and [^{11}C]SCH23390 studies. L-[β-^{11}C]DOPA studies were conducted without L-DOPA decarboxylase inhibitor premedication.

PET procedures

All PET studies were performed with a Siemens ECAT Exact HR+ system, which provides 63 sections with an axial field of view of 15.5 cm (Brix et al., 1997). The intrinsic spatial resolution was 4.3 mm in-plane and 4.2 mm full-width at half maximum (FWHM) axially. With a Hanning filter (cutoff frequency: 0.4 cycle/pixel), the reconstructed in-plane resolution was 7.5 mm FWHM. Data were acquired in three-dimensional mode. Scatter was corrected (Watson et al., 1996). A head fixation device with thermoplastic attachments for individual fit minimized head movement during PET measurements. A 10-min transmission scan using a ^{68}Ge-^{68}Ga line source was performed for correction of attenuation. After intravenous rapid bolus injection of [^{11}C]raclopride, [^{11}C]FLB457, or [^{11}C]PE2I, data were acquired for 90 min in a consecutive series of time frames. For [^{11}C]SCH23390 and L-[β-^{11}C]DOPA studies, data were acquired for 60 and 89 min after intravenous rapid bolus injection, respectively. The frame sequence consisted of twelve 20-s frames, sixteen 1-min frames, ten 4-min frames, and five 6-min frames for [^{11}C]raclopride, and nine 20-s frames, five 1-min frames, four 2-min frames, eleven 4-min frames, and six 5-min frames for [^{11}C]FLB457 and [^{11}C]PE2I. For [^{11}C]SCH23390, the frame sequence consisted of thirty 2-min frames. The frame sequence for L-[β-^{11}C]DOPA studies consisted of seven 1-min frames, five 2-min frames, four 3-min frames, and twelve 5-min. Injected radioactivity was 197–235 MBq, 213–239 MBq, 212–242 MBq, 197–230 MBq, and 320–402 MBq for [^{11}C]SCH23390, [^{11}C]raclopride, [^{11}C]FLB457, [^{11}C]PE2I, and L-[β-^{11}C]DOPA, respectively. Specific radioactivity was 23–81 GBq/μmol, 133–285 GBq/μmol, 72–371 GBq/μmol, 55–1103 GBq/μmol, and 29–82 GBq/μmol at the time of injection for [^{11}C]SCH23390, [^{11}C]raclopride, [^{11}C]FLB457, [^{11}C]PE2I, and L-[β-^{11}C]DOPA, respectively.

Table 1
Number of subjects per study and average age

Study	Number of subjects	Age (years, mean±SD)
[^{11}C]SCH23390	10	27.3±4.6
[^{11}C]raclopride	10	26.9±3.9
[^{11}C]FLB457	10	26.9±3.9
[^{11}C]PE2I	10	24.2±3.1
L-[β-^{11}C]DOPA	10	23.4±3.3

All subjects are male.
[^{11}C]raclopride and [^{11}C]FLB457 PET were conducted on same subjects.
Two subjects underwent L-[β-^{11}C]DOPA, [^{11}C]raclopride, and [^{11}C]FLB457 studies; one underwent L-[β-^{11}C]DOPA and [^{11}C]SCH23390 studies.

MR imaging procedures

All MR imaging studies were performed with a 1.5-T MR scanner (Philips Medical Systems, Best, The Netherlands). Three-dimensional volumetric acquisition of a T1-weighted gradient echo sequence produced a gapless series of thin transverse sections (TE: 9.2 ms; TR: 21 ms; flip angle: 30°; field of view: 256 mm; acquisition matrix: 256×256; slice thickness: 1 mm).

Calculation of parametric images

For PET studies with [^{11}C]SCH23390, [^{11}C]raclopride, [^{11}C]FLB457, and [^{11}C]PE2I, binding potential (BP) was calculated by the reference tissue model method on a voxel-by-voxel basis (Lammertsma et al., 1996; Lammertsma and Hume, 1996). By this method, the time–activity curve in the brain region is described by that in the reference region with no specific binding, assuming that both regions have the same level of nondisplaceable radioligand binding:

$$C_i(t) = R_1 \cdot C_r(t) + \{k_2 - R_1 \cdot k_2/(1+\mathrm{BP})\} \cdot C_r(t) \otimes \exp\{-k_2 \cdot t/(1+\mathrm{BP})\}.$$

where C_i is the radioactivity concentration in a brain region; $C_r(t)$ is the radioactivity concentration in the reference region. R_1 is the ratio of K_1/K_1' (K_1, influx rate constant for the brain region, K_1', influx rate constant for the reference region). k_2 is the efflux rate constant for the brain region, and ⊗ denotes the convolution integral. In this analysis, three parameters (BP, R_1, and k_2) were estimated by the basis function method (Cselenyi et al., 2006; Gunn et al., 1997). The cerebellum was used as a reference region. We used in-house written software to calculate parametric images.

For the L-[β-^{11}C]DOPA study, the dopamine synthesis index (I) was calculated on a voxel-by-voxel basis as follows (Dhawan et al., 2002; Hoshi et al., 1993; Ito et al., 2007):

$$I = \frac{\int_{t_1}^{t_2} C_i(t)\mathrm{d}t}{\int_{t_1}^{t_2} C_i'(t)\mathrm{d}t} - 1$$

where C_i is the radioactivity concentration in a brain region, and C_i' is the radioactivity concentration in a brain region with no

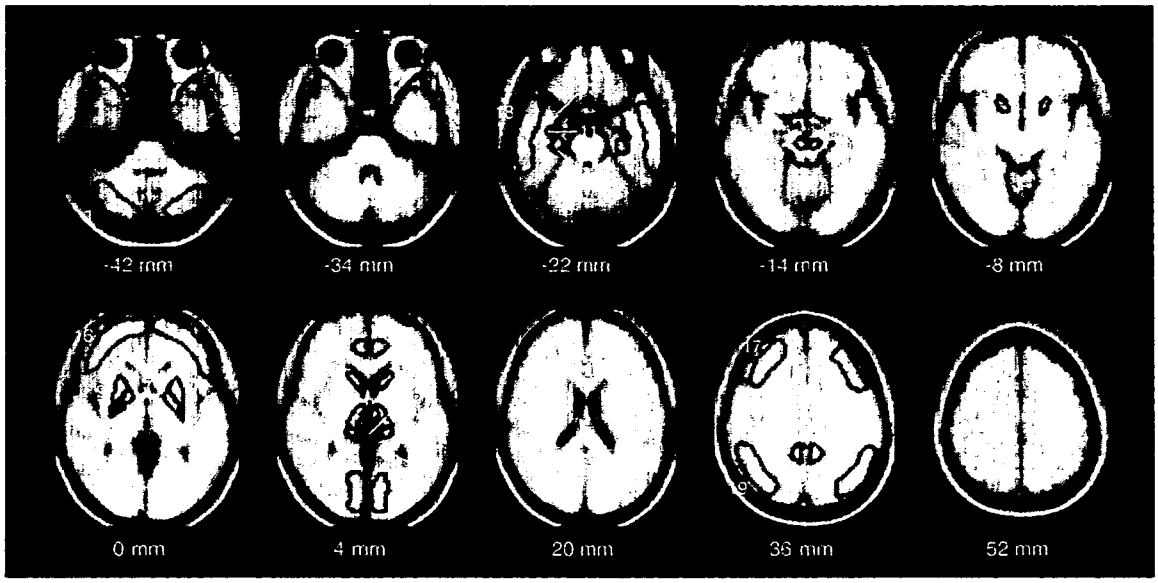

Fig. 1. Regions of interest drawn on all anatomically standardized images (1: cerebellum, 2: substantia nigra, 3: thalamus, 4: anterior nuclei, 5: dorsomedial nucleus, 6: pulvinar, 7: caudate head, 8: nucleus accumbens, 9: putamen, 10: globus pallidus, 11: hippocampus, 12: parahippocampal gyrus, 13: uncus, 14: anterior part of the cingulate gyrus, 15: posterior part of the cingulate gyrus, 16: base side of frontal cortex, 17: convexity side of frontal cortex, 18: lateral side of temporal cortex, 19: parietal cortex, 20: cuneus of occipital cortex). All images are transaxial sections parallel to the anterior-posterior commissure (AC–PC) line. The slice positions are −42, −34, −22, −14, −8, 0, 4, 20, 36 and 52 mm from the AC–PC line.

irreversible binding. The occipital cortex was used as a region with no irreversible binding, as this region is known to have the lowest dopamine concentration (Brown et al., 1979) and lowest aromatic L-amino acid decarboxylase activity (Lloyd and Hornykiewicz, 1972). Integration intervals (t_1 to t_2) of 29 to 89 min, representing late portions of the time–activity curves, were used (Ito et al., 2006b).

Data analysis

All MR images were coregistered to the PET images with the statistical parametric mapping (SPM2) system (Friston et al., 1990). MR images were transformed into the standard brain size and shape by linear and nonlinear parameters by SPM2 (anatomic standardization). The brain templates used in SPM2 for anatomic standardization were T1 templates for MR images, i.e., Montreal Neurological Institute (MNI)/International Consortium for Brain Mapping (ICBM) 152 T1 templates as supplied with SPM2. All PET images were also transformed into the standard brain size and shape by using the same parameters as the MR images. Thus, brain images of all subjects had the same anatomic format. Gray matter, white matter, and cerebrospinal fluid images were segmented and extracted from all anatomically standardized MR images by applying voxel-based morphometry methods with the SPM2 system (Ashburner and Friston, 2000). These segmented MR images indicate the tissue fraction of gray or white matter per voxel (mL/mL). All anatomically standardized PET, gray matter and white matter images were smoothed with an 8-mm FWHM isotropic Gaussian kernel, because final spatial resolution of PET camera was approximately 8 mm FWHM.

Regions of interest (ROIs) were drawn on all anatomically standardized PET, gray matter and white matter images with reference to the T1-weighted MR image (Fig. 1). ROIs were defined for the cerebellar cortex, substantia nigra with ventral tegmental area, thalamus and its subregions (anterior nuclei, dorsomedial nucleus, and pulvinar) (Okubo et al., 1999; Yasuno et al., 2004), caudate head, nucleus accumbens, putamen, globus pallidus, hippocampus, posterior part of parahippocampal gyrus, uncus including amygdala, anterior and posterior parts of the cingulate gyrus, base and convexity sides of frontal cortex, lateral side of temporal cortex, parietal cortex, and cuneus of occipital cortex,

Table 2
Representative MNI coordinates in ROIs drawn on anatomically standardized images

Region	Right			Left		
	X	*Y*	*Z*	*X*	*Y*	*Z*
Cerebellum	30	−74	−42	−30	−74	−42
Substantia nigra	6	−20	−14	−6	−20	−42
Thalamus	11	−18	4	−11	−18	4
AN	5	−12	4	−5	−12	4
DMN	8	−22	4	−8	−22	4
PUL	14	−29	4	−14	−29	4
Caudate head	12	16	4	−12	16	4
Nucleus accumbens	17	13	−8	−18	12	−8
Putamen	24	9	0	−24	7	0
Globus pallidus	19	0	0	−18	−2	0
Hippocampus	31	−12	−22	−30	−13	−22
Parahippocampal gyrus	28	−21	−22	−28	−23	−22
Uncus	21	−3	−22	−22	−2	−22
Anterior cingulate	7	44	4	−7	45	4
Posterior cingulate	8	−47	36	−8	−47	36
Frontal base	35	56	0	−34	56	0
Frontal convexity	35	31	36	−36	27	36
Lateral temporal cortex	59	−11	−22	−58	−13	−22
Parietal cortex	45	−62	36	−45	−65	36
Occipital cuneus	10	−81	4	−8	−81	4

AN: anterior nuclei, DMN: dorsomedial nucleus, PUL: pulvinar in the thalamus.

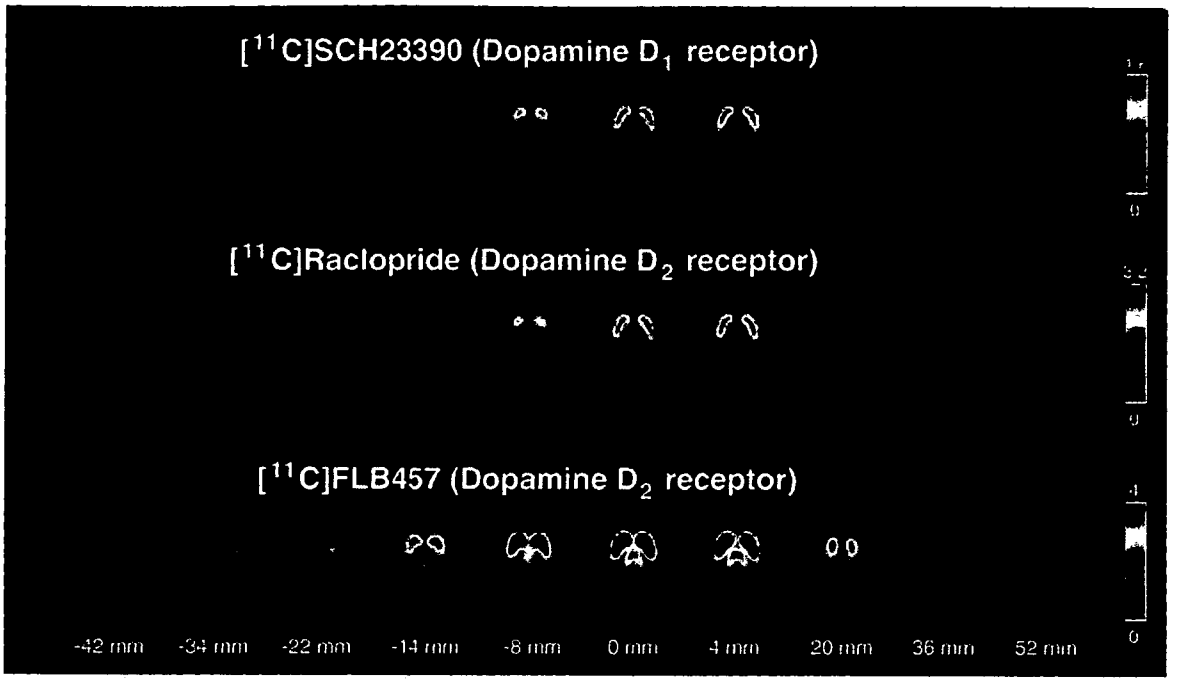

Fig. 2. Anatomically standardized averaged PET images obtained with [^{11}C]SCH23390, [^{11}C]raclopride, and [^{11}C]FLB457. All images are transaxial sections parallel to the AC–PC line. The slice positions are −42, −34, −22, −14, −8, 0, 4, 20, 36, and 52 mm from the AC–PC line. The anterior is at the top of the image and the subjects' right is at the left. Scale maximum and minimum values are 1.6 and 0 of BP for [^{11}C]SCH23390, 3.2 and 0 of BP for [^{11}C]raclopride, and 4 and 0 of BP for [^{11}C]FLB457, respectively.

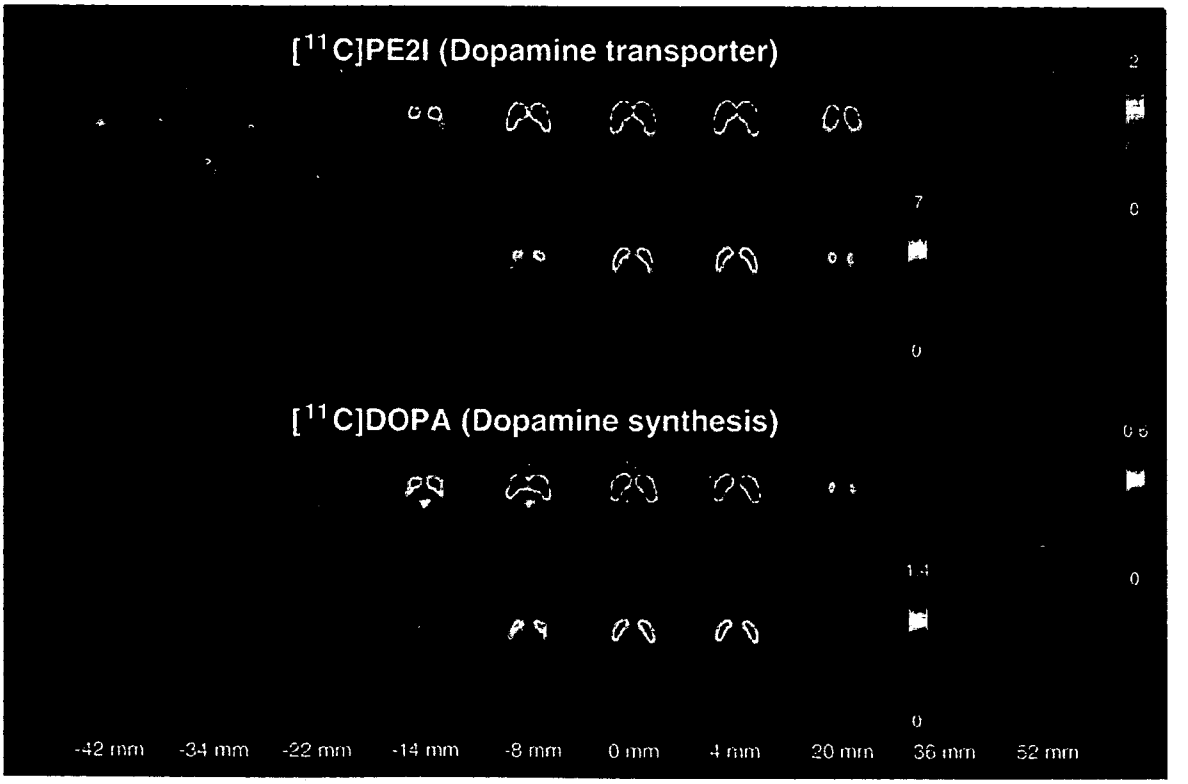

Fig. 3. Anatomically standardized averaged PET images obtained with [^{11}C]PE2I and L-[β-^{11}C]DOPA. All images are transaxial sections parallel to the AC-PC line. The slice positions are −42, −34, −22, −14, −8, 0, 4, 20, 36, and 52 mm from the AC–PC line. The anterior is at the top of the image and the subjects' right is at the left. Scale maximum and minimum values are 7 or 2 and 0 of BP for [^{11}C]PE2I, and 1.4 or 0.6 and 0 of *I* for L-[β-^{11}C]DOPA, respectively.

considering regional distribution of dopaminergic neurotransmission system. Representative MNI coordinates in ROIs (approximations of the arithmetic center of ROIs) are given in Table 2.

To compare BP and *I* values between tracers for each ROI, percentages of the putamen of BP or *I* were calculated for [^{11}C]SCH23390, [^{11}C]PE2I, and L-[β-^{11}C]DOPA, because the putamen showed highest BP and *I* values among all brain regions for all tracers. Since [^{11}C]FLB457 is not favorable for estimating striatal BP values, the percentage of BP of the putamen in the extrastriatal regions was calculated as the percentage of the putaminal BP values for [^{11}C]raclopride mediated with thalamic BP values:

$$\%\ \text{of putamen in extrastriatal regions} = \frac{\text{Extrastriatum(FLB)}}{\text{Putamen(Racl.)}} \bullet \frac{\text{Thalamus(Racl.)}}{\text{Thalamus(FLB)}}$$

where Extrastriatum(FLB) is BP in the extrastriatal regions for [^{11}C]FLB457, Putamen(Racl.) is BP in the putamen for [^{11}C]raclopride, and Thalamus(Racl.) and Thalamus(FLB) are BP in the thalamus for [^{11}C]raclopride and [^{11}C]FLB457 studies, respectively. Although [^{11}C]raclopride binding in the extrastriatal regions is low (Farde et al., 1988), it has been reported that the specific binding of [^{11}C]raclopride in the thalamus was low but detectable (Ito et al., 1999). In these calculation, values without the partial volume correction (see below) were used.

Partial volume correction

BP and *I* values are affected by the regional gray matter fraction because of the limited spatial resolution of the PET scanner. The BP and *I* values per gray matter fraction in an ROI for cerebellar and cerebral cortical regions can be calculated as BP or *I* divided by the gray matter fraction obtained from segmented MR images for each ROI (Ito et al., 2006a).

Results

Anatomically standardized averaged images of BP and *I* are shown in Figs. 2 and 3, respectively. The BP and *I* values of each ROI for [^{11}C]SCH23390, [^{11}C]raclopride, [^{11}C]FLB457, [^{11}C]PE2I, and L-[β-^{11}C]DOPA are given in Table 3. Percentages of the putamen for BP or *I* values of [^{11}C]SCH23390, [^{11}C]FLB457, [^{11}C]PE2I, and L-[β-^{11}C]DOPA are shown in Fig. 4. In the substantia nigra with ventral tegmental area, binding to dopamine D_2 receptors, but very low binding to D_1 receptors, was observed. In the striatum, greatest bindings to dopamine D_1, D_2 receptors and transporters as well as the highest dopamine synthesis were observed. For the limbic regions, relatively high bindings of dopamine D_2 receptors were observed in the uncus. Relatively high dopamine synthesis was observed in the uncus and anterior part of the cingulate gyrus. For the other neocortical regions, the highest binding to dopamine D_2 receptors was observed in the temporal cortex. D_1 receptor binding among the neocortical regions was uniformly observed. Binding to dopamine transporter was very low in the neocortical regions. In the thalamus, relatively high binding to dopamine D_2 receptors was observed, but binding to D_1 receptors was very low.

Anatomically standardized averaged T1-weighted MR images and averaged images of gray and white matter fractions are shown in Fig. 5. The tissue fraction values of gray and white matter per voxel in cerebellar and cerebral cortices are given in Table 4, and the BP and *I* values with correction for the gray matter fraction in an ROI are shown in Table 5. Almost the same order of BP and *I* values among cerebral cortical regions was observed between before and after the correction for the gray matter fraction.

Discussion

A normal database for pre and postsynaptic dopaminergic neurotransmission components, including the striatal and extra-

Table 3
Average binding potential (BP) and dopamine synthesis index (*I*) values

Region	BP				*I*
	[^{11}C]SCH23390	[^{11}C]raclopride	[^{11}C]FLB457	[^{11}C]PE2I	L-[β-^{11}C]DOPA
Cerebellum	–	–	–	–	0.09±0.05
Substantia nigra	0.01±0.06	0.20±0.07	1.72±0.26	0.82±0.12	0.33±0.08
Thalamus	0.08±0.06	0.38±0.05	2.80±0.40	0.29±0.08	0.12±0.07
AN	0.07±0.08	0.42±0.10	3.84±0.51	0.30±0.08	0.20±0.13
DMN	0.04±0.06	0.32±0.07	3.04±0.52	0.20±0.09	0.11±0.08
PUL	0.09±0.07	0.38±0.06	2.24±0.41	0.21±0.09	0.12±0.09
Caudate head	1.13±0.24	2.21±0.22	6.69±0.94	5.84±1.00	0.79±0.17
Nucleus accumbens	1.20±0.23	2.19±0.38	6.73±1.11	4.75±0.70	0.94±0.14
Putamen	1.39±0.24	2.84±0.30	7.97±1.15	6.22±0.90	1.20±0.16
Globus pallidus	0.83±0.23	1.80±0.25	5.57±0.91	3.38±0.72	0.74±0.13
Hippocampus	0.20±0.09	0.27±0.06	1.42±0.24	0.10±0.05	0.16±0.09
Parahippocampal gyrus	0.18±0.10	0.25±0.05	1.30±0.22	−0.01±0.03	0.14±0.09
Uncus	0.17±0.07	0.26±0.05	1.84±0.26	0.09±0.06	0.19±0.07
Anterior cingulate	0.34±0.11	0.31±0.07	0.93±0.16	0.16±0.05	0.22±0.05
Posterior cingulate	0.41±0.11	0.36±0.05	1.01±0.36	0.14±0.07	0.12±0.04
Frontal base	0.25±0.08	0.25±0.04	0.75±0.20	0.09±0.03	0.07±0.06
Frontal convexity	0.30±0.08	0.27±0.04	0.70±0.18	0.13±0.05	0.07±0.05
Lateral temporal cortex	0.31±0.07	0.32±0.04	1.61±0.30	0.03±0.02	0.12±0.05
Parietal cortex	0.29±0.10	0.29±0.02	1.02±0.35	0.11±0.04	0.04±0.04
Occipital cuneus	0.37±0.10	0.29±0.05	0.50±0.27	0.12±0.04	–

Values are shown as mean±SD.
AN: anterior nuclei, DMN: dorsomedial nucleus, PUL: pulvinar in the thalamus.

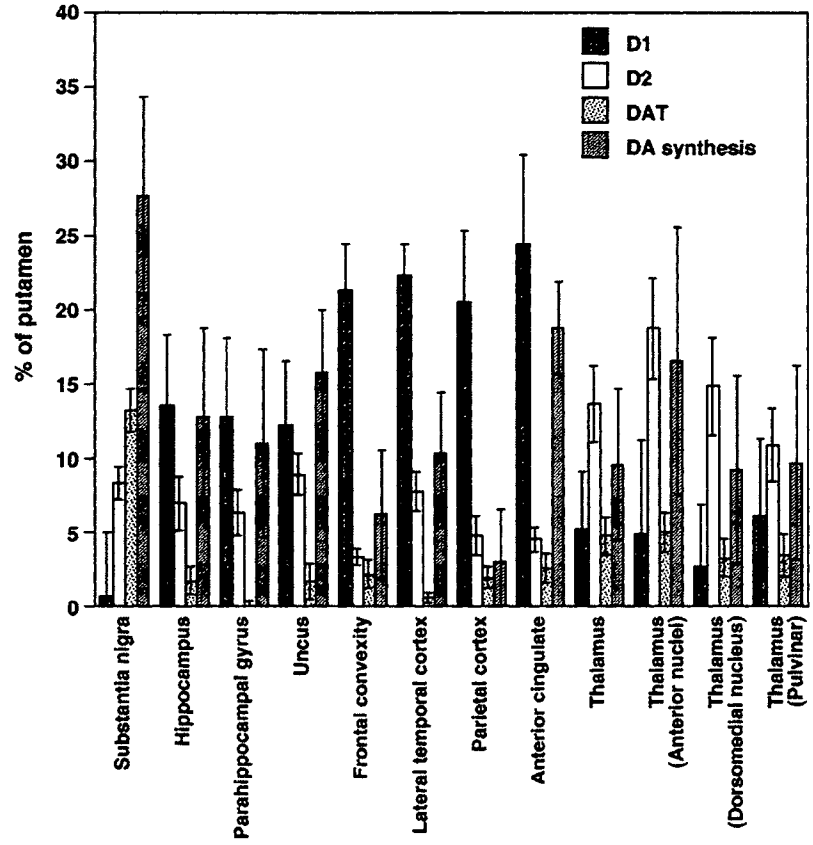

Fig. 4. Percentage of the putamen for BP or *I* values of [^{11}C]SCH23390 (dopamine D_1 receptor), [^{11}C]FLB457 (dopamine D_2 receptor), [^{11}C]PE2I (dopamine transporter (DAT)), and L-[β-^{11}C]DOPA (dopamine (DA) synthesis) for the substantia nigra, hippocampus, parahippocampal gyrus, uncus, frontal convexity, lateral temporal cortex, parietal cortex, anterior cingulate, thalamus and its subregions (anterior nuclei, dorsomedial nucleus, and pulvinar). Values are mean ± SD.

striatal dopamine D_1 and D_2 receptor bindings, dopamine transporter binding, and endogenous dopamine synthesis in the living human brain could be constructed by making use of the anatomic standardization technique. Although the subjects all differed in terms of the database (dopamine D_1, D_2 receptor, transporter, and synthesis), the anatomic standardization technique allowed us to compare between regional distributions of each dopaminergic neurotransmission component in vivo. While partial volume effects cause systemic underestimations of BP and *I* values, the partial volume correction did not change the order of BP and *I* values among cerebral cortical regions. This database is expected to be useful for various researches to understand the physiology of dopaminergic functions in the living human brain; however, regional differences in test-retest reliability in PET measurements should be considered (Hirvonen et al., 2001; Sudo et al., 2001). In addition, it has been reported that the reference tissue model method with the basis function method might cause overestimation and underestimation of BP in regions with low and high BP, respectively (Cselenyi et al., 2006; Gunn et al., 1997). Since BP values calculated from measured data may show some bias depending on kinetic models and calculation methods, it is not obvious if calculated BP values linearly reflect the biological pre- and postsynaptic functions. Thus, there might be some limitations in comparison of regional distributions between tracers using percentages of the putamen. This database can also be used in the investigation of regional abnormalities of dopaminergic neurotransmission in neuropsychiatric disorders, if database will be constructed from a large number of subjects. It might be difficult to use our database in other PET center due to between-center differences in data acquisition protocols, image reconstruction process, quantification methods, etc. (Ito et al., 2004). To solve these differences, further studies were required.

Nigrostriatal dopaminergic system

Midbrain

The ascending projections from the dopaminergic neurons in the substantia nigra to the striatum compose the nigrostriatal dopaminergic system (Bentivoglio and Morelli, 2005). Binding to dopamine D_2 receptors in the midbrain including the substantia nigra and ventral tegmental area was observed to be the same in the living human brain as in human postmortem studies (Hall et al., 1996; Joyce et al., 1991), suggesting the existence of receptors in dopaminergic neurons. On the other hand, no binding to dopamine D_1 receptors was observed in this region. These observations support the finding that dopaminergic autoreceptors in the midbrain are mainly of D_2 type (Meador-Woodruff et al., 1994; Morelli et al., 1987). In the living human brain, dopamine synthesis in the midbrain was greater than in the cerebral neocortical regions, although the aromatic L-amino acid decarboxylase activity in the substantia nigra was almost the same as in the parietal and occipital cortices in the human postmortem brain (Lloyd and Hornykiewicz, 1972). A medium amount of dopamine transporter was also found in the

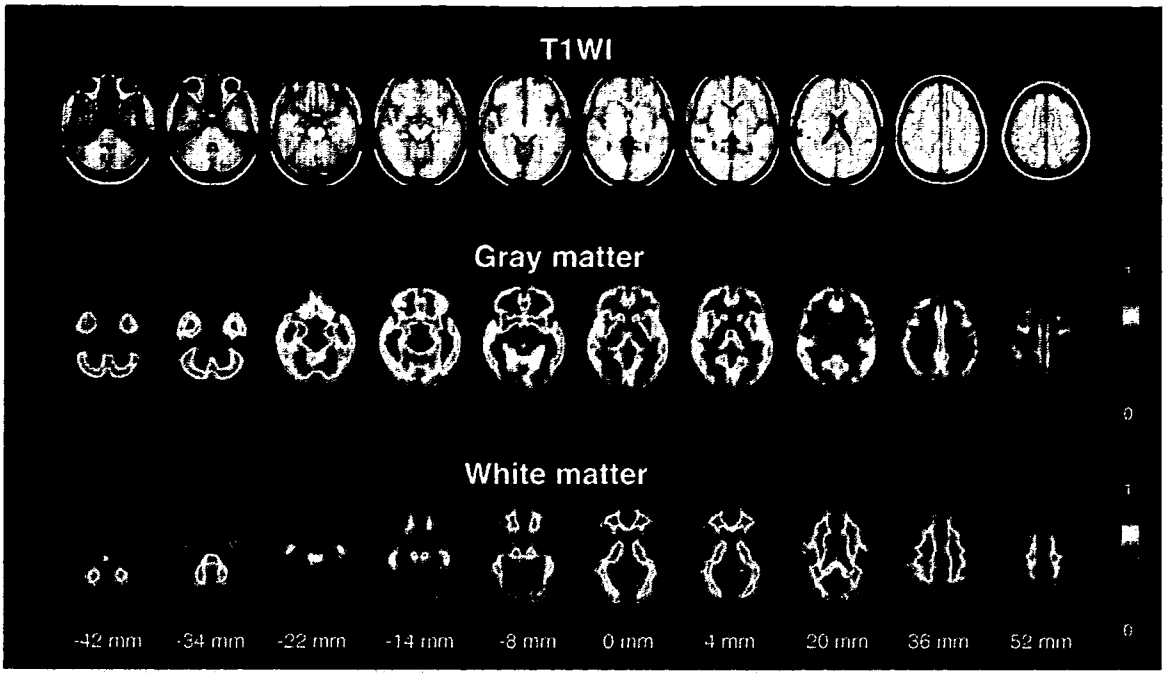

Fig. 5. Anatomically standardized averaged T1-weighted MR images and averaged images of gray and white matter fractions. All images are transaxial sections parallel to the AC–PC line. The slice positions are −42, −34, −22, −14, −8, 0, 4, 20, 36, and 52 mm from the AC–PC line. The anterior is at the top of the image and the subjects' right is at the left. Scale maximum and minimum values for gray and white matter images are 1 and 0 of gray and white matter fractions (mL/mL), respectively. T1WI, T1-weighted image.

midbrain, similar to a human postmortem study (Hall et al., 1999) and animal studies (Boja et al., 1994; Ciliax et al., 1995).

Striatum

The highest bindings to dopamine D_1 and D_2 receptors were observed in the striatum among the all brain regions, indicating the highest density of receptors, the same as reported in human postmortem studies (Hall et al., 1994). The highest binding to dopamine transporter in the striatum was also observed, indicating the highest transporter density (Boja et al., 1994; Ciliax et al., 1995; Hall et al., 1999). These findings indicate that this region is rich in dopaminergic synapses. Although the microdistribution of dopamine D_2 receptors in the striatum is differential with D_2 predominating in the striosomes and D_1 in the matrix (Joyce et al., 1986), the distributions of dopamine D_1 and D_2 receptor bindings appeared almost uniform in the striatum on account of the limited spatial resolution of the PET scanner. The highest dopamine synthesis was also observed in the striatum. This finding is in good agreement with previous studies showing the highest aromatic L-amino acid decarboxylase activity (Lloyd and Hornykiewicz, 1972) and the highest dopamine concentration in the striatum (Brown et al., 1979). These findings, in total, reflect the dense dopamine innervation of this region from the substantia nigra (Moore et al., 2003).

Globus pallidus

In the globus pallidus, higher bindings to dopamine D_1 and D_2 receptors as compared with other extrastriatal regions were observed, much the same as in human postmortem studies (Hall et al., 1996, 1994). These findings support the concept of the dopaminergic pallidal projections from neurons in the substantia nigra and ventral tegmental area (Bentivoglio and Morelli, 2005; Parent et al., 1990). In addition, it has been reported that binding to dopamine D_2 receptors in the external segment of the pallidum was higher than that in the internal segment in the human postmortem brain (Hall et al., 1996; Joyce et al., 1991). However, spillover from striatal radioactivity owing to the limited spatial resolution of the PET scanner might hamper an accurate estimation of pallidal binding. BP values of [^{11}C]raclopride in the globus pallidus and nucleus accumbens were different from previous study of the living human brain (Ito et al., 1999). These differences might be caused by differences in anatomic standardization techniques, methods of calculation of BP, image reconstruction process, PET cameras, etc.

Mesocorticolimbic dopaminergic system

Limbic system

The ascending projections from dopaminergic neurons in the ventral tegmental area to the cerebral cortices and limbic system compose the mesocorticolimbic dopaminergic system (Bentivoglio and Morelli, 2005). The ventral striatum, the so-called limbic striatum, including the nucleus accumbens is also innervated by the ventral tegmental area (Bentivoglio and Morelli, 2005; Joel and Weiner, 2000).

Relatively high bindings of dopamine D_2 receptors were observed in the uncus including the amygdala, parahippocampal gyrus, and hippocampus as compared with cerebral neocortical regions. These distributions are in good agreement with those found in human postmortem studies (Hall et al., 1996, 1994; Joyce et al., 1991). It has been reported that densities of dopamine D_2 receptors in the hippocampus are lower than in the amygdala and parahippocampal gyrus (Hall et al., 1996, 1994). The present study also

Table 4
Average tissue fractions of gray and white matter per voxel in cerebellar and cerebral cortices (mL/mL)

Region	Tissue fraction	
	Gray matter	White matter
Cerebellum	0.75±0.04	0.16±0.03
Hippocampus	0.80±0.04	0.14±0.03
Parahippocampal gyrus	0.74±0.03	0.19±0.03
Uncus	0.83±0.03	0.03±0.01
Anterior cingulate	0.65±0.04	0.20±0.03
Posterior cingulate	0.72±0.04	0.18±0.05
Frontal base	0.55±0.02	0.29±0.02
Frontal convexity	0.57±0.04	0.29±0.04
Lateral temporal cortex	0.66±0.02	0.25±0.02
Parietal cortex	0.55±0.03	0.35±0.03
Occipital cuneus	0.64±0.04	0.27±0.04

Values are shown as mean±SD.

showed lower binding of dopamine D_2 receptors in the hippocampus than in the uncus. A human postmortem study showed aromatic L-amino acid decarboxylase activity in the amygdala but not in the hippocampus (Lloyd and Hornykiewicz, 1972). In the present study, dopamine synthesis was observed in the hippocampus in addition to the uncus including amygdala and parahippocampal gyrus although the spatial resolution of the PET scanner was limited. The present results might indicate the dopaminergic innervation to the hippocampus in addition to the amygdala and the parahippocampal gyrus (Joyce and Murray, 1994). As for the other extrastriatal regions, bindings to dopamine transporter were very low (Hall et al., 1999).

The anterior part of the cingulate gyrus representing the limbic system has projections from the dopaminergic neurons in the ventral tegmental area, and connections with hippocampal regions. In this region, bindings to dopamine D_1 and D_2 receptors similar to those in neocortical regions were observed. Binding to dopamine transporter was very low in this region, as in neocortical regions. It should be noted that dopamine synthesis was relatively higher in the anterior cingulate than in neocortical regions.

Neocortex

In the cerebral neocortical regions, binding to dopamine D_2 receptors was found to be low comparing with the other brain regions as previous studies of the living human brain (Okubo et al., 1999) and postmortem brain (Hall et al., 1996, 1994; Joyce et al., 1991; Lidow et al., 1989) have also reported. Regional differences in D_2 receptor binding among the neocortical regions were observed in the living human brain as in the human postmortem brain (Hall et al., 1996, 1994; Joyce et al., 1991), i.e., highest binding in the temporal cortex and lowest binding in the occipital cortex. Binding to dopamine D_2 receptors was higher in the parietal cortex than in the frontal and occipital cortices. Binding to dopamine D_1 receptors in the cerebral neocortical regions as compared with the striatum was higher than that to D_2 receptors as shown in a previous human postmortem study (Hall et al., 1994). Using the present database of dopamine D_1 and D_2 receptors, it could be observed that regional distribution of D_1 receptor binding among the neocortical regions was more uniform as compared with that to D_2 receptors. Percentages of the putamen for BP of dopamine D_2 receptors in the cerebral neocortical regions were around 5–10% in the present study, whereas those were reported to be about 1% in a previous human postmortem study with [^{125}I]epidepride (Hall et al., 1996). This discrepancy might be caused by the difference in used radioligands. The difference between in vivo and in vitro conditions might also cause such discrepancy.

In the present study, the binding to dopamine transporter was almost negligible level in the cerebral neocortical regions, as also reported in a human postmortem study (Hall et al., 1999), although both dopamine D_1 and D_2 receptors exist in these regions. These data indicate that released dopamine in the dopaminergic synapse might be inactivated by enzymatic degradation rather than by reuptake to the transporter (Hall et al., 1999). In addition, dopamine reuptake through the norepinephrine transporter in cerebral cortical regions with low levels of the dopamine transporter was observed in mice (Moron et al., 2002). Dopamine synthesis was observed in the cerebral neocortical regions except the occipital cortex. Among these regions, highest and lowest dopamine synthesis was observed in the temporal and frontal cortex, respectively. This regional difference in dopamine synthesis was in good agreement with that in aromatic L-amino acid decarboxylase activity (Lloyd and Hornykiewicz, 1972). In the temporal cortex, highest dopamine synthesis and highest dopamine D_2 receptor binding were observed among the neocortical regions. On the other hand, it should be noted that the parietal cortex showed relatively low dopamine synthesis and relatively high dopamine D_2 receptor binding as compared with the frontal cortex.

In the present study, database were constructed from male subjects. However, it has been reported that a gender difference in

Table 5
Average binding potential (BP) and dopamine synthesis index (*I*) values with correction for gray matter fraction in an ROI

Region	BP				*I*
	[^{11}C]SCH23390	[^{11}C]raclopride	[^{11}C]FLB457	[^{11}C]PE2I	L-[β-^{11}C]DOPA
Cerebellum	–	–	–	–	0.12±0.06
Hippocampus	0.24±0.11	0.34±0.07	1.77±0.33	0.12±0.06	0.20±0.12
Parahippocampal gyrus	0.25±0.13	0.33±0.07	1.75±0.30	−0.01±0.04	0.18±0.12
Uncus	0.21±0.08	0.31±0.06	2.22±0.31	0.11±0.07	0.23±0.08
Anterior cingulate	0.53±0.16	0.47±0.10	1.41±0.24	0.24±0.08	0.34±0.06
Posterior cingulate	0.57±0.11	0.50±0.06	1.38±0.47	0.20±0.10	0.17±0.05
Frontal base	0.45±0.13	0.46±0.07	1.35±0.37	0.16±0.05	0.13±0.11
Frontal convexity	0.52±0.13	0.46±0.07	1.18±0.29	0.24±0.10	0.12±0.08
Lateral temporal cortex	0.47±0.11	0.47±0.06	2.39±0.40	0.05±0.03	0.18±0.08
Parietal cortex	0.53±0.16	0.52±0.05	1.80±0.60	0.21±0.06	0.06±0.08
Occipital cuneus	0.58±0.15	0.45±0.07	0.78±0.40	0.18±0.06	–

Values are shown as mean±SD.

dopamine D_2 receptor binding was observed in the frontal cortex (Kaasinen et al., 2001). Further studies to investigate gender differences in pre- and postsynaptic dopaminergic neurotransmission components using database would be required.

Thalamic dopaminergic system

The dopaminergic projections to the thalamus from neurons in the hypothalamus, periaqueductal gray matter, ventral mesencephalon, and the lateral parabrachial nucleus were reported (Sanchez-Gonzalez et al., 2005). Therefore, a dopaminergic system targeting the thalamus, which might be independent from the nigrostriatal dopaminergic system and the mesocorticolimbic dopaminergic system, has been proposed (Sanchez-Gonzalez et al., 2005). In the present study, relatively high binding to dopamine D_2 receptors was observed in the thalamus. In particular, anterior nuclei and dorsomedial nucleus showed higher binding in the present study, the same as reported by previous studies of the living human brain (Okubo et al., 1999) and human postmortem brain (Hall et al., 1996; Rieck et al., 2004). On the other hand, binding to dopamine D_1 receptors was very low (Hall et al., 1994). Binding to dopamine transporter was very low in the thalamus, the same as in the postmortem study (Hall et al., 1999), although dopamine D_2 receptors exist in this region. This means that released dopamine in the thalamic dopaminergic synapse might be inactivated by enzymatic degradation, the same as reported in other extrastriatal regions (Hall et al., 1999). Although aromatic L-amino acid decarboxylase activity in the thalamus has been reported to be very low (Lloyd and Hornykiewicz, 1972), dopamine synthesis in this region was observed in the living human brain, supporting the existence of dopaminergic innervation in the thalamus.

In conclusion, we have built a normal database of pre- and postsynaptic dopaminergic neurotransmission components in the living human brain using PET and the anatomic standardization technique. This database enables us to compare regional distributions of striatal and extrastriatal dopamine D_1 and D_2 receptor bindings, dopamine transporter binding, and endogenous dopamine synthesis. This database is expected to be useful for various researches to understand the physiology of dopaminergic functions in the living human brain. This database can also be used in the investigation of regional abnormalities of dopaminergic neurotransmission in neuropsychiatric disorders.

Acknowledgments

This study was supported in part by a Grant-in-Aid for Molecular Imaging Program from the Ministry of Education, Culture, Sports, Science and Technology (MEXT), Japanese Government and a Grant-in-Aid for Scientific Research (C) (No. 18591372) from the Japan Society for the Promotion of Science. We thank Mr. Katsuyuki Tanimoto, Mr. Takahiro Shiraishi, and Mr. Akira Ando for their assistance in performing the PET experiments at the National Institute of Radiological Sciences. We also thank Ms. Yoshiko Fukushima of the National Institute of Radiological Sciences for her help as clinical research coordinator.

References

Ashburner, J., Friston, K.J., 2000. Voxel-based morphometry—the methods. NeuroImage 11, 805–821.

Bentivoglio, M., Morelli, M., 2005. The organization and circuits of mesencephalic dopaminergic neurons and the distribution of dopamine receptors in the brain. In: Dunnett, S.B., Bentivoglio, M., Bjorklund, A., Hokfelt, T. (Eds.), Handbook of Chemical Neuroanatomy. Dopamine, vol. 21. Elsevier, Amsterdam, pp. 1–107.

Boja, J.W., Vaughan, R., Patel, A., Shaya, E.K., Kuhar, M.J., 1994. The dopamine transporter. In: Niznik, H.B. (Ed.), Dopamine Receptors and Transporters. Marcel Dekker, Inc., New York, pp. 611–644.

Brix, G., Zaers, J., Adam, L.E., Bellemann, M.E., Ostertag, H., Trojan, H., Haberkorn, U., Doll, J., Oberdorfer, F., Lorenz, W.J., 1997. Performance evaluation of a whole-body PET scanner using the NEMA protocol. J. Nucl. Med. 38, 1614–1623.

Brown, R.M., Crane, A.M., Goldman, P.S., 1979. Regional distribution of monoamines in the cerebral cortex and subcortical structures of the rhesus monkey: concentrations and in vivo synthesis rates. Brain Res. 168, 133–150.

Ciliax, B.J., Heilman, C., Demchyshyn, L.L., Pristupa, Z.B., Ince, E., Hersch, S.M., Niznik, H.B., Levey, A.I., 1995. The dopamine transporter: immunochemical characterization and localization in brain. J. Neurosci. 15, 1714–1723.

Cselenyi, Z., Olsson, H., Halldin, C., Gulyas, B., Farde, L., 2006. A comparison of recent parametric neuroreceptor mapping approaches based on measurements with the high affinity PET radioligands [^{11}C] FLB 457 and [^{11}C]WAY 100635. NeuroImage 32, 1690–1708.

Dhawan, V., Ma, Y., Pillai, V., Spetsieris, P., Chaly, T., Belakhlef, A., Margouleff, C., Eidelberg, D., 2002. Comparative analysis of striatal FDOPA uptake in Parkinson's disease: ratio method versus graphical approach. J. Nucl. Med. 43, 1324–1330.

Emond, P., Garreau, L., Chalon, S., Boazi, M., Caillet, M., Bricard, J., Frangin, Y., Mauclaire, L., Besnard, J.C., Guilloteau, D., 1997. Synthesis and ligand binding of nortropane derivatives: *N*-substituted 2beta-carbomethoxy-3beta-(4′-iodophenyl)nortropane and *N*-(3-iodoprop-(2E)-enyl)-2beta-carbomethoxy-3beta-(3′,4′-disubstituted phenyl) nortropane. New high-affinity and selective compounds for the dopamine transporter. J. Med. Chem. 40, 1366–1372.

Farde, L., Ehrin, E., Eriksson, L., Greitz, T., Hall, H., Hedstrom, C.G., Litton, J.E., Sedvall, G., 1985. Substituted benzamides as ligands for visualization of dopamine receptor binding in the human brain by positron emission tomography. Proc. Natl. Acad. Sci. U. S. A. 82, 3863–3867.

Farde, L., Halldin, C., Stone-Elander, S., Sedvall, G., 1987a. PET analysis of human dopamine receptor subtypes using ^{11}C-SCH 23390 and ^{11}C-raclopride. Psychopharmacology 92, 278–284.

Farde, L., Wiesel, F.A., Hall, H., Halldin, C., Stone-Elander, S., Sedvall, G., 1987b. No D_2 receptor increase in PET study of schizophrenia. Arch. Gen. Psychiatry 44, 671–672.

Farde, L., Pauli, S., Hall, H., Eriksson, L., Halldin, C., Hogberg, T., Nilsson, L., Sjogren, I., Stone-Elander, S., 1988. Stereoselective binding of ^{11}C-raclopride in living human brain—a search for extrastriatal central D2-dopamine receptors by PET. Psychopharmacology 94, 471–478.

Farde, L., Wiesel, F.A., Stone-Elander, S., Halldin, C., Nordstrom, A.L., Hall, H., Sedvall, G., 1990. D_2 dopamine receptors in neuroleptic-naive schizophrenic patients. A positron emission tomography study with [^{11}C]raclopride. Arch. Gen. Psychiatry 47, 213–219.

Farde, L., Halldin, C., Muller, L., Suhara, T., Karlsson, P., Hall, H., 1994. PET study of [^{11}C]b-CIT binding to monoamine transporters in the monkey and human brain. Synapse 16, 93–103.

Fox, P.T., Mintun, M.A., Reiman, E.M., Raichle, M.E., 1988. Enhanced detection of focal brain responses using intersubject averaging and change-distribution analysis of subtracted PET images. J. Cereb. Blood Flow Metab. 8, 642–653.

Friston, K.J., Frith, C.D., Liddle, P.F., Dolan, R.J., Lammertsma, A.A., Frackowiak, R.S., 1990. The relationship between global and local changes in PET scans. J. Cereb. Blood Flow Metab. 10, 458–466.

Gjedde, A., 1988. Exchange diffusion of large neutral amino acids between blood and brain. In: Rakic, L., Begley, D.J., Davson, H., Zlokovic, B.V. (Eds.), Peptide and Amino Acid Transport Mechanisms in the Cerebral Nervous System. Stockton Press, New York, pp. 209–217.

Gjedde, A., Reith, J., Dyve, S., Leger, G., Guttman, M., Diksic, M., Evans, A., Kuwabara, H., 1991. Dopa decarboxylase activity of the living human brain. Proc. Natl. Acad. Sci. U. S. A. 88, 2721–2725.

Gunn, R.N., Lammertsma, A.A., Hume, S.P., Cunningham, V.J., 1997. Parametric imaging of ligand-receptor binding in PET using a simplified reference region model. NeuroImage 6, 279–287.

Hall, H., Sedvall, G., Magnusson, O., Kopp, J., Halldin, C., Farde, L., 1994. Distribution of D_1- and D_2-dopamine receptors, and dopamine and its metabolites in the human brain. Neuropsychopharmacology 11, 245–256.

Hall, H., Farde, L., Halldin, C., Hurd, Y.L., Pauli, S., Sedvall, G., 1996. Autoradiographic localization of extrastriatal D_2-dopamine receptors in the human brain using [^{125}I]epidepride. Synapse 23, 115–123.

Hall, H., Halldin, C., Guillotcau, D., Chalon, S., Emond, P., Besnard, J., Farde, L., Sedvall, G., 1999. Visualization of the dopamine transporter in the human brain postmortem with the new selective ligand [^{125}I]PE2I. NeuroImage 9, 108–116.

Halldin, C., Stone-Elander, S., Farde, L., Ehrin, E., Fasth, K.J., Langstrom, B., Sedvall, G., 1986. Preparation of ^{11}C-labelled SCH 23390 for the in vivo study of dopamine D-1 receptors using positron emission tomography. International Journal of Radiation Applications and Instrumentation—Part A. Appl. Radiat. Isotopes 37, 1039–1043.

Halldin, C., Farde, L., Hogberg, T., Mohell, N., Hall, H., Suhara, T., Karlsson, P., Nakashima, Y., Swahn, C.G., 1995. Carbon-11-FLB 457: a radioligand for extrastriatal D_2 dopamine receptors. J. Nucl. Med. 36, 1275–1281.

Halldin, C., Foged, C., Chou, Y.H., Karlsson, P., Swahn, C.G., Sandell, J., Sedvall, G., Farde, L., 1998. Carbon-11-NNC 112: a radioligand for PET examination of striatal and neocortical D1-dopamine receptors. J. Nucl. Med. 39, 2061–2068.

Hartvig, P., Agren, H., Reibring, L., Tedroff, J., Bjurling, P., Kihlberg, T., Langstrom, B., 1991. Brain kinetics of L-[β-^{11}C]dopa in humans studied by positron emission tomography. J. Neural Transm. Gen. Sect. 86, 25–41.

Hietala, J., Syvalahti, E., Vuorio, K., Rakkolainen, V., Bergman, J., Haaparanta, M., Solin, O., Kuoppamaki, M., Kirvela, O., Ruotsalainen, U., Salokangas, R.K.R., 1995. Presynaptic dopamine function in striatum of neuroleptic-naive schizophrenic patients. Lancet 346, 1130–1131.

Hirvonen, J., Nagren, K., Kajander, J., Hietala, J., 2001. Measurement of cortical dopamine D_1 receptor binding with [^{11}C]SCH23390: a test-retest analysis. J. Cereb. Blood Flow Metab. 21, 1146–1150.

Hoshi, H., Kuwabara, H., Leger, G., Cumming, P., Guttman, M., Gjedde, A., 1993. 6-[^{18}F]fluoro-L-DOPA metabolism in living human brain: a comparison of six analytical methods. J. Cereb. Blood Flow Metab. 13, 57–69.

Huang, S.C., Yu, D.C., Barrio, J.R., Grafton, S., Melega, W.P., Hoffman, J.M., Satyamurthy, N., Mazziotta, J.C., Phelps, M.E., 1991. Kinetics and modeling of L-6-[^{18}F]fluoro-dopa in human positron emission tomographic studies. J. Cereb. Blood Flow Metab. 11, 898–913.

Ito, H., Hietala, J., Blomqvist, G., Halldin, C., Farde, L., 1998. Comparison of the transient equilibrium and continuous infusion method for quantitative PET analysis of [^{11}C]raclopride binding. J. Cereb. Blood Flow Metab. 18, 941–950.

Ito, H., Okubo, Y., Halldin, C., Farde, L., 1999. Mapping of central D_2 dopamine receptors in man using [^{11}C]raclopride: PET with anatomic standardization technique. NeuroImage 9, 235–242.

Ito, H., Sudo, Y., Suhara, T., Okubo, Y., Halldin, C., Farde, L., 2001. Error analysis for quantification of [^{11}C]FLB 457 binding to extrastriatal D_2 dopamine receptors in the human brain. NeuroImage 13, 531–539.

Ito, H., Kanno, I., Kato, C., Sasaki, T., Ishii, K., Ouchi, Y., Iida, A., Okazawa, H., Hayashida, K., Tsuyuguchi, N., Kuwabara, Y., Senda, M., 2004. Database of normal human cerebral blood flow, cerebral blood volume, cerebral oxygen extraction fraction and cerebral metabolic rate of oxygen measured by positron emission tomography with ^{15}O-labelled carbon dioxide or water, carbon monoxide and oxygen: a multicentre study in Japan. Eur. J. Nucl. Med. Mol. Imaging 31, 635–643.

Ito, H., Inoue, K., Goto, R., Kinomura, S., Taki, Y., Okada, K., Sato, K., Sato, T., Kanno, I., Fukuda, H., 2006a. Database of normal human cerebral blood flow measured by SPECT: I. Comparison between I-123-IMP, Tc-99m-HMPAO, and Tc-99m-ECD as referred with O-15 labeled water PET and voxel-based morphometry. Ann. Nucl. Med. 20, 131–138.

Ito, H., Ota, M., Ikoma, Y., Seki, C., Yasuno, F., Takano, A., Maeda, J., Nakao, R., Suzuki, K., Suhara, T., 2006b. Quantitative analysis of dopamine synthesis in human brain using positron emission tomography with L-[β-^{11}C]DOPA. Nucl. Med. Commun. 27, 723–731.

Ito, H., Shidahara, M., Takano, H., Takahashi, H., Nozaki, S., Suhara, T., 2007. Mapping of central dopamine synthesis in man using positron emission tomography with L-[β-^{11}C]DOPA. Ann. Nucl. Med. 21, 355–360.

Joel, D., Weiner, I., 2000. The connections of the dopaminergic system with the striatum in rats and primates: an analysis with respect to the functional and compartmental organization of the striatum. Neuroscience 96, 451–474.

Joyce, J.N., Murray, A., 1994. Distribution of D_1- and D_2-like dopamine receptors in human brain. In: Niznik, H.B. (Ed.), Dopamine Receptors and Transporters. Marcel Dekker, Inc., New York, pp. 345–381.

Joyce, J.N., Sapp, D.W., Marshall, J.F., 1986. Human striatal dopamine receptors are organized in compartments. Proc. Natl. Acad. Sci. U. S. A. 83, 8002–8006.

Joyce, J.N., Janowsky, A., Neve, K.A., 1991. Characterization and distribution of [^{125}I]epidepride binding to dopamine D_2 receptors in basal ganglia and cortex of human brain. J. Pharmacol. Exp. Ther. 257, 1253–1263.

Kaasinen, V., Nagren, K., Hietala, J., Farde, L., Rinne, J.O., 2001. Sex differences in extrastriatal dopamine D_2-like receptors in the human brain. Am. J. Psychiatry 158, 308–311.

Kohler, C., Hall, H., Ogren, S.O., Gawell, L., 1985. Specific in vitro and in vivo binding of ^{3}H-raclopride. A potent substituted benzamide drug with high affinity for dopamine D-2 receptors in the rat brain. Biochem. Pharmacol. 34, 2251–2259.

Laakso, A., Vilkman, H., Alakare, B., Haaparanta, M., Bergman, J., Solin, O., Peurasaari, J., Rakkolainen, V., Syvalahti, E., Hietala, J., 2000. Striatal dopamine transporter binding in neuroleptic-naive patients with schizophrenia studied with positron emission tomography. Am. J. Psychiatry 157, 269–271.

Lammertsma, A.A., Hume, S.P., 1996. Simplified reference tissue model for PET receptor studies. NeuroImage 4, 153–158.

Lammertsma, A.A., Bench, C.J., Hume, S.P., Osman, S., Gunn, K., Brooks, D.J., Frackowiak, R.S., 1996. Comparison of methods for analysis of clinical [^{11}C]raclopride studies. J. Cereb. Blood Flow Metab. 16, 42–52.

Laruelle, M., 1998. Imaging dopamine transmission in schizophrenia. A review and meta-analysis. Q. J. Nucl. Med. 42, 211–221.

Laruelle, M., Abi-Dargham, A., van Dyck, C., Gil, R., D'Souza, D.C., Krystal, J., Scibyl, J., Baldwin, R., Innis, R., 2000. Dopamine and serotonin transporters in patients with schizophrenia: an imaging study with [^{123}I]b-CIT. Biol. Psychiatry 47, 371–379.

Lidow, M.S., Goldman-Rakic, P.S., Rakic, P., Innis, R.B., 1989. Dopamine D_2 receptors in the cerebral cortex: distribution and pharmacological characterization with [^{3}H]raclopride. Proc. Natl. Acad. Sci. U. S. A. 86, 6412–6416.

Lindstrom, L.H., Gefvert, O., Hagberg, G., Lundberg, T., Bergstrom, M., Hartvig, P., Langstrom, B., 1999. Increased dopamine synthesis rate in medial prefrontal cortex and striatum in schizophrenia indicated by L-(β-^{11}C) DOPA and PET. Biol. Psychiatry 46, 681–688.

Lloyd, K.G., Hornykiewicz, O., 1972. Occurrence and distribution of aromatic L-amino acid (L-DOPA) decarboxylase in the human brain. J. Neurochem. 19, 1549–1559.

Meador-Woodruff, J.H., Damask, S.P., Watson Jr., S.J., 1994. Differential expression of autoreceptors in the ascending dopamine systems of the human brain. Proc. Natl. Acad. Sci. U. S. A. 91, 8297–8301.

Moore, R.Y., Whone, A.L., McGowan, S., Brooks, D.J., 2003. Monoamine

neuron innervation of the normal human brain: an ^{18}F-DOPA PET study. Brain Res. 982, 137–145.

Morelli, M., Carboni, E., Devoto, S., Di Chiara, G., 1987. 6-Hydroxydopamine lesions reduce specific [^{3}H]sulpiride binding in the rat substantia nigra: direct evidence for the existence of nigral D-2 autoreceptors. Eur. J. Pharmacol. 140, 99–104.

Moron, J.A., Brockington, A., Wise, R.A., Rocha, B.A., Hope, B.T., 2002. Dopamine uptake through the norepinephrine transporter in brain regions with low levels of the dopamine transporter: evidence from knock-out mouse lines. J. Neurosci. 22, 389–395.

Muller, L., Halldin, C., Farde, L., Karlsson, P., Hall, H., Swahn, C.G., Neumeyer, J., Gao, Y., Milius, R., 1993. [^{11}C] β-CIT, a cocaine analogue. Preparation, autoradiography and preliminary PET investigations. Nucl. Med. Biol. 20, 249–255.

Nagano, A.S., Ito, K., Kato, T., Arahata, Y., Kachi, T., Hatano, K., Kawasumi, Y., Nakamura, A., Yamada, T., Abe, Y., Ishigaki, T., 2000. Extrastriatal mean regional uptake of fluorine-18-FDOPA in the normal aged brain-an approach using MRI-aided spatial normalization. NeuroImage 11, 760–766.

Nordstrom, A.L., Farde, L., Eriksson, L., Halldin, C., 1995. No elevated D_2 dopamine receptors in neuroleptic-naive schizophrenic patients revealed by positron emission tomography and [^{11}C]*N*-methylspiperone. Psychiatry Res. 61, 67–83.

Okubo, Y., Olsson, H., Ito, H., Lofti, M., Suhara, T., Halldin, C., Farde, L., 1999. PET mapping of extrastriatal D_2-like dopamine receptors in the human brain using an anatomic standardization technique and [^{11}C]FLB 457. NeuroImage 10, 666–674.

Parent, A., Lavoie, B., Smith, Y., Bedard, P., 1990. The dopaminergic nigropallidal projection in primates: distinct cellular origin and relative sparing in MPTP-treated monkeys. Adv. Neurol. 53, 111–116.

Reith, J., Benkelfat, C., Sherwin, A., Yasuhara, Y., Kuwabara, H., Andermann, F., Bachneff, S., Cumming, P., Diksic, M., Dyve, S.E., Etienne, P., Evans, A.C., Lal, S., Shevell, M., Savard, G., Wong, D.F., Chouinard, G., Gjedde, A., 1994. Elevated dopa decarboxylase activity in living brain of patients with psychosis. Proc. Natl. Acad. Sci. U. S. A. 91, 11651–11654.

Rieck, R.W., Ansari, M.S., Whetsell Jr., W.O., Deutch, A.Y., Kessler, R.M., 2004. Distribution of dopamine D_2-like receptors in the human thalamus: autoradiographic and PET studies. Neuropsychopharmacology 29, 362–372.

Sanchez-Gonzalez, M.A., Garcia-Cabezas, M.A., Rico, B., Cavada, C., 2005. The primate thalamus is a key target for brain dopamine. J. Neurosci. 25, 6076–6083.

Sudo, Y., Suhara, T., Inoue, M., Ito, H., Suzuki, K., Saijo, T., Halldin, C., Farde, L., 2001. Reproducibility of [^{11}C]FLB 457 binding in extrastriatal regions. Nucl. Med. Commun. 22, 1215–1221.

Suhara, T., Sudo, Y., Okauchi, T., Maeda, J., Kawabe, K., Suzuki, K., Okubo, Y., Nakashima, Y., Ito, H., Tanada, S., Halldin, C., Farde, L., 1999. Extrastriatal dopamine D_2 receptor density and affinity in the human brain measured by 3D PET. Int. J. Neuropsychopharmacol. 2, 73–82.

Suhara, T., Okubo, Y., Yasuno, F., Sudo, Y., Inoue, M., Ichimiya, T., Nakashima, Y., Nakayama, K., Tanada, S., Suzuki, K., Halldin, C., Farde, L., 2002. Decreased dopamine D_2 receptor binding in the anterior cingulate cortex in schizophrenia. Arch. Gen. Psychiatry 59, 25–30.

Tedroff, J., Aquilonius, S.M., Hartvig, P., Lundqvist, H., Bjurling, P., Langstrom, B., 1992. Estimation of regional cerebral utilization of [^{11}C]-L-3,4-dihydroxy-phenylalanine (DOPA) in the primate by positron emission tomography. Acta Neurol. Scand. 85, 166–173.

Watson, C.C., Newport, D., Casey, M.E., 1996. A single scatter simulation technique for scatter correction in 3D PET. In: Grangeat, P., Amans, J.L. (Eds.), Three-Dimensional Image Reconstruction in Radiology and Nuclear Medicine. Kluwer Academic Publishers, Dordrecht, The Netherlands, pp. 255–268.

Yasuno, F., Suhara, T., Okubo, Y., Sudo, Y., Inoue, M., Ichimiya, T., Takano, A., Nakayama, K., Halldin, C., Farde, L., 2004. Low dopamine D_2 receptor binding in subregions of the thalamus in schizophrenia. Am. J. Psychiatry 161, 1016–1022.

Cerebral Cortex Advance Access published January 17, 2008

Cerebral Cortex
doi:10.1093/cercor/bhm214

Neural Correlates of Human Virtue Judgment

Hidehiko Takahashi[1,2], Motoichiro Kato[3], Masato Matsuura[2], Michihiko Koeda[4], Noriaki Yahata[5], Tetsuya Suhara[1] and Yoshiro Okubo[4]

[1]Department of Molecular Neuroimaging, National Institute of Radiological Sciences, 9-1, 4-chome, Anagawa, Inage-ku, Chiba 263-8555, Japan, [2]Department of Life Sciences and Bio-informatics, Graduate School of Health Sciences, Tokyo Medical and Dental University, 1-5-45 Yushima Bunkyo-ku Tokyo, Japan, [3]Department of Neuropsychiatry, Keio University School of Medicine, 35 Shinanomachi, Shinjuku-ku, Tokyo, Japan, [4]Department of Neuropsychiatry and [5]Department of Pharmacology, Nippon Medical School, 1-1-5, Sendagi, Bunkyo-ku, Tokyo, Japan

Neuroimaging studies have demonstrated that the brain regions implicated in moral cognition. However, those studies have focused exclusively on violation of social norms and negative moral emotions, and very little effort has been expended on the investigation of positive reactions to moral excellence. It remains unclear whether the brain regions implicated in moral cognition have specific roles in processing moral violation or, more generally, process human morality per se. Using functional magnetic resonance imaging, brain activations during evaluation of moral beauty and depravity were investigated. Praiseworthiness for moral beauty was associated with activation in the orbitofrontal cortex, whereas blameworthiness for moral depravity was related to the posterior superior temporal sulcus. Humans might have developed different neurocognitive systems for evaluating blameworthiness and praiseworthiness. The central process of moral beauty evaluation might be related to that of aesthetic evaluation. Our finding might contribute to a better understanding of human morality.

Keywords: blameworthiness, moral, orbitofrontal cortex, praiseworthiness, superior temporal sulcus, virtue

Introduction

The emerging field of cognitive neuroscience is providing new insights into the neural basis of moral cognition and behaviors. As David Hume (1978) and Adam Smith (1976) already noted in the 18th century, some contemporary philosophers have emphasized the importance of emotion and intuition in moral judgment, although moral reasoning could contribute to moral judgment (Haidt 2001; Greene and Haidt 2002). Supporting this view, recent neuroimaging studies and brain lesion studies have demonstrated that emotion-related brain regions such as the posterior superior temporal sulcus (pSTS), medial prefrontal cortex (MPFC), orbitofrontal cortex (OFC), and amygdala play important roles in moral judgment (Damasio 2000; Greene and Haidt 2002; Takahashi et al. 2004; Moll et al. 2005). Previous psychological as well as neuroimaging studies mainly focused on violation of social norms and negative moral emotions such as guilt or embarrassment (Greene and Haidt 2002; Haidt 2003a, 2003b; Takahashi et al. 2004; Moll et al. 2005; Mobbs et al. 2007). Morals are standards or principles of right or wrong behaviors and the goodness or badness of human character. It remains unclear whether the brain regions implicated in moral cognition are specialized in processing immorality, that is, negative deviance from social norms or, more generally, processing deviance from social standards regardless of whether the stimuli positively or negatively deviate from them. There has been very little study on positive moral emotions or psychological responses to moral beauty, but with the advent of the positive psychology movement (Seligman and Csikszentmihalyi 2000), researchers have started to focus on positive moral emotions. Many people experience spontaneous pleasure when they can help others without any expectation of reward. Neuroimaging studies suggest that cooperative behaviors might be psychologically rewarding (Rilling et al. 2002; de Quervain et al. 2004; Moll et al. 2006). It is also human nature that we are easily and strongly moved by people who are cooperating with others. Haidt (2003a, 2003b) started to call an emotion elicited by others' act of virtue or moral beauty as "elevation." When people observe others' virtuous, commendable acts, they feel warm, pleasant, and "tingling" feelings and are motivated to help others and to become better people themselves. Hume (1978) wrote that "a generous and noble character never fails to charm and delight us" and Smith (1976) noted that "man desires, not only praise, but praiseworthiness." We also could have an aesthetic feeling in human virtuous acts and be often attracted by the beauty itself (Haidt 2003a). However, there are very few studies to have concentrated on this aspect of moral beauty. According to Haidt (2003a), we cannot have a full understanding of human morality until we can explain why and how people are so powerfully affected by the sight of a stranger helping another stranger.

For the evolution and persistence of cooperation, it is necessary for humans to detect cheaters and cooperators. Otherwise, selfish strategies will eliminate cooperative strategies (Axelrod and Hamilton 1981; Cosmides and Tooby 1992). Cosmides and Tooby (1992) argued that humans have evolved neurocognitive systems that specialize in detecting "cheating," violation of social contracts, and that produce a feeling that those who violate social norms should be blamed and punished. In fact, functional magnetic resonance imaging (fMRI) studies reported activation in brain regions such as pSTS and MPFC during detection of violation of social contracts (Canessa et al. 2005; Fiddick et al. 2005). On the other hand, it is also argued that humans have evolved a neurocognitive system that skillfully assesses the cooperativeness of others (Price 2006), and empirical evidence suggests that people will cooperate with those whom they have observed cooperating with others (Wedekind and Milinski 2000; Milinski et al. 2002). However, there is as yet no documented study regarding the investigation

of the neural correlates during the observance of praiseworthy, virtuous acts of others.

In this study, we investigated the brain activation associated with the judgment of moral beauty, virtue, comparing it with that of moral depravity, vice. We hypothesized that the judgment of moral beauty and depravity would show different brain activation patterns. Specifically, moral depravity would be linked to brain regions, such as pSTS and MPFC, and moral beauty would recruit the brain regions implicated in positive emotions, such as OFC.

Materials and Methods

Participants

Fifteen healthy volunteers (mean age 20.1 years, standard deviation [SD] = 0.8) participated in this study. All subjects were Japanese and right-handed. The participants were free of any criteria for neuropsychiatric disorders based on unstructured psychiatric screening interviews. None of the participants were taking alcohol at the time nor did they have a history of psychiatric disorder, significant physical illness, head injury, neurological disorder, or alcohol or drug dependence. All participants underwent an MRI to rule out cerebral anatomic abnormalities. After complete explanation of the study, written informed consent was obtained from all participants and the study was approved by the Institutional Ethics Committee.

Materials

Three types of short sentences were provided (neutral, moral beauty, and moral depravity). Each sentence was written in Japanese and in the 3rd person. Sentences of moral depravity were expressing moral violation, and those of moral beauty were expressing acts like charity, self-sacrifice, altruism, humanitarianism, and so on. Neutral sentences were expected to express no prominent emotional content. In order to validate our expected results, we conducted an initial survey. We prepared 30–35 sentences for each of 3 conditions (neutral, moral beauty, and moral depravity). Forty-two other healthy volunteers (21 males and 21 females, mean age 22.5 years, SD = 3.3) than the subjects participating in this fMRI study were screened. Using 7-point Likert scales, they read and rated each sentence in terms of morality/immorality (−3 = extremely immoral, 0 = neither moral nor immoral, and 3 = extremely moral) and praiseworthiness/blameworthiness (−3 = extremely blameworthy, 0 = neither praiseworthy nor blameworthy, and 3 = extremely praiseworthy). Based on the initial survey, we selected 18 sentences for each of the 3 conditions. These sentences are shown in Supplementary Table S1. The sentences were projected via a computer and a telephoto lens onto a screen mounted on a head coil. The subjects were instructed to read the sentences silently and were told to imagine the events described in the sentences. They were also told that they should rate the sentences according to how moral/immoral or praiseworthy/blameworthy the events were. After reading each sentence, the subjects were instructed to press a selection button with the right index finger, indicating that they had read and understood it. The experimental design consisted of 6 blocks for each of the 3 conditions (neutral, moral beauty, and moral depravity) interleaved with 20-s rest periods. We used a block design rather than an event-related design as it is difficult to obtain sufficient understandable stimuli, that is, depictions of moral beauty and depravity are difficult to parse rapidly (Luo et al. 2006). The order of presentation for the 3 conditions was randomized. During the rest condition, participants viewed a crosshair pattern projected to the center of the screen. In each 24-s block, 3 different sentences of the same condition were presented for 8 s each. Using 7-point Likert scales, the participants rated each sentence in terms of morality/immorality and praiseworthiness/blameworthiness after the scans.

Image Acquisition

Images were acquired with a 1.5 Tesla Signa system (General Electric, Milwaukee, WI). Functional images of 203 volumes were acquired with T2*-weighted gradient echo planar imaging sequences sensitive to blood oxygenation level-dependent contrast. Each volume consisted of 40 transaxial contiguous slices with a slice thickness of 3 mm to cover almost the whole brain (flip angle, 90°; time echo [TE], 50 ms; time repetition [TR], 4 s; matrix, 64 × 64; and field of view, 24 × 24 cm). High-resolution, T1-weighted anatomic images were acquired for anatomic comparison (124 contiguous axial slices, 3-dimensional Spoiled-Grass sequence, slice thickness 1.5 mm; TE, 9 ms; TR, 22 ms; flip angle, 30°; matrix, 256 × 192; and field of view, 25 × 25 cm).

Analysis of Functional Imaging Data

Data analysis was performed with statistical parametric mapping software package (SPM02) (Wellcome Department of Cognitive Neurology, London, UK) running with MATLAB (Mathworks, Natick, MA). All volumes were realigned to the 1st volume of each session to correct for subject motion and were spatially normalized to the standard space defined by the Montreal Neurological Institute template. After normalization, all scans had a resolution of 2 × 2 × 2 mm^3. Functional images were spatially smoothed with a 3-dimensional isotropic Gaussian kernel (full width at half maximum of 8 mm). Low frequency noise was removed by applying a high-pass filter (cutoff period = 192 s) to the fMRI time series at each voxel. A temporal smoothing function was applied to the fMRI time series to enhance the temporal signal-to-noise ratio. Significant hemodynamic changes for each condition were examined using the general linear model with boxcar functions convolved with a hemodynamic response function. Statistical parametric maps for each contrast of the *t*-statistic were calculated on a voxel-by-voxel basis.

To assess the specific condition effect, we used the contrasts of the moral beauty minus neutral (MB − N) and moral depravity minus neutral (MD − N). A random effects model, which estimates the error variance for each condition across the subjects, was implemented for group analysis. This procedure provides a better generalization for the population from which data are obtained. The contrast images were obtained from single-subject analysis and entered into the group analysis. A 1-sample *t*-test was applied to determine group activation for each effect. We used SPM's small volume correction to correct for multiple testing in regions about which we had a priori hypothesis. These a priori volumes of interest (VOIs) included the pSTS, MPFC, and OFC. VOIs for pSTS (angular gyrus), MPFC (superior and medial frontal gyrus), and OFC (inferior frontal gyrus) were defined by standardized VOI templates implemented in brain atlas software (Maldjian et al. 2003). Significant activations surviving this correction at $P < 0.05$ are reported. We describe activations outside regions of interest surviving a threshold of $P < 0.001$, uncorrected, with an extent threshold of 10 contiguous voxels. To assess common activation in MB − N and MD conditions, we conducted a conjunction analysis of MB − N and MD − N contrasts at the 2nd level.

We conducted regression analysis to demonstrate a more direct link between regional brain activities with the subjective judgments of praiseworthiness and blameworthiness. Using the mean of the ratings of praiseworthiness and blameworthiness for each subject as the covariate, regression analysis with the contrasts (MB − N and MD − N) and the covariate was performed at the 2nd level. The masks of MB − N and MD − N contrasts from the 1-sample *t*-test ($P < 0.001$) were applied to confine the regions where significant activations were observed. Using the effect sizes, representing the percent signal change, of the contrasts (MB − N and MD − N) at the peak coordinates uncovered by regression analysis, we plotted the fMRI signal changes and ratings of praiseworthiness and blameworthiness.

Results

Initial Survey

As we predicted, neutral sentences were judged neither moral/praiseworthy nor immoral/blameworthy. The averages of the ratings of morality/immorality and praiseworthiness/blameworthiness for neutral sentences were 0.0 (SD = 0.1) and 0.0 (SD = 0.1), respectively. The average of ratings of morality and

praiseworthiness for 18 sentences of moral beauty were 2.3 (SD = 0.8) and 1.8 (SD = 0.9), respectively. The average of ratings of immorality and blameworthiness for 18 sentences of moral depravity were -2.4 (SD = 0.7) and -2.1 (SD = 0.8), respectively.

Self Rating

The self-rating results of the subjects participating in the fMRI study were comparable to the results obtained in the initial survey. The averages of the ratings of morality/immorality and praiseworthiness/blameworthiness for neutral sentences were 0.1 (SD = 0.2) and 0.0 (SD = 0.1), those of morality and praiseworthiness for sentences of moral beauty were 2.5 (SD = 0.3) and 2.1 (SD = 0.5), and those of immorality and blameworthiness for sentences of moral depravity were -2.4 (SD = 0.3) and -2.1 (SD = 0.4), respectively. Self-ratings of immorality were correlated with blameworthiness ($r = 0.58$, $P = 0.025$), and those of morality were correlated with praiseworthiness ($r = 0.68$, $P = 0.005$).

fMRI Result

The MB-N condition produced activations in the left OFC, left dorsal lateral prefrontal cortex (DLPFC), left supplementary motor area (SMA), left temporal pole, and visual cortex, (Table 1 and Fig. 1*A*). The MD - N condition produced activations in the left pSTS and MPFC (Table 1 and Fig. 1*B*). The activations in a priori regions (pSTS, MPFC, and OFC) survived a threshold of $P < 0.05$ corrected for multiple comparisons across a small VOI. A conjunction analysis of MB - N and MD - N contrast revealed no significant activations.

Regression analysis revealed positive linear correlations between self-rating of praiseworthiness and the degree of activation in the left OFC ($x = -38$, $y = 28$, and $z = -20$) in MB - N contrast (Figs 2*A* and 3*A*). There were correlations between self-rating of blameworthiness and the degree of activation in the left pSTS ($x = -54$, $y = -66$, and $z = 28$) in MD - N contrast (Figs 2*B* and 3*B*). Theses correlations in a priori regions (pSTSC and OFC) survived a threshold of $P < 0.05$ corrected for multiple comparisons across a small VOI.

Discussion

This study has demonstrated that the brain activations during evaluation of positive deviance from the moral standard, moral beauty, showed different patterns from those of negative deviance, moral depravity. In line with previous reports, moral depravity conditions relative to neutral condition produced greater activity in the left pSTS and MPFC, the components of neural substrates that have been suggested to be involved in human moral cognition (Takahashi et al. 2004; Moll et al. 2005). A novel finding in this study was that moral beauty conditions relative to neutral condition produced greater activity in the left frontal regions, such as OFC, DLPFC, and SMA. This means that the regions suggested to play important roles in moral cognition are more specialized in processing moral violation and do not cover human morality per se.

Although self-ratings of immorality were correlated with blameworthiness and those of morality were correlated with praiseworthiness, empirical evidence suggests that blameworthiness for immoral acts and praiseworthiness for commendable or cooperative acts were not symmetrical. In other words, blameworthiness for impulsive immoral acts without deliberate intention was discounted compared with deliberate immoral acts, whereas praiseworthiness for commendable acts was not discounted regardless of whether the positive acts were impulsive or deliberate (Pizarro et al. 2003). This is also common in legal culpability. This means that people tend to link blameworthiness to intention and the process of wrongdoing, whereas they tend to link praiseworthiness to outcomes of positive acts regardless of deliberate intention or not.

Table 1
Brain activations in moral beauty condition and moral depravity condition relative to neutral condition

Brain region	L/R	Coordinates			*Z*-score
		x	*y*	*z*	
Moral beauty-neutral					
Visual cortex	L/R	14	−90	−8	4.59
OFC*	L	−40	32	−20	3.39
Temporal pole	L	−50	18	−24	3.51
SMA	L	−48	0	48	3.52
DLPFC	L	−52	26	14	3.30
Moral depravity-neutral					
MPFC*	L/R	6	58	14	4.35
pSTS*	L	−54	−64	30	3.40

Note: Coordinates and *Z*-score refer to the peak of each brain region. L, left; R, right. All values, $P < 0.001$, uncorrected. *$P < 0.05$, corrected for multiple comparisons across a small VOI.

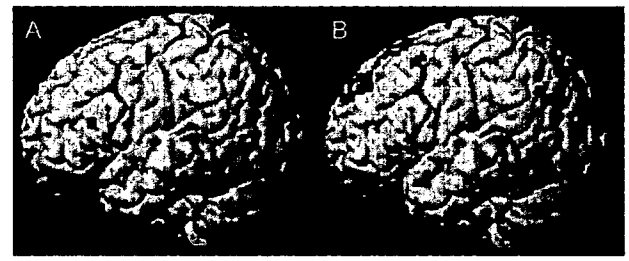

Figure 1. Images showing brain activations in response to (*A*) MB − N condition and (*B*) MD − N condition. (*A*) Significant activation in OFC is shown. (*B*) Significant activations in MPFC and pSTS are shown.

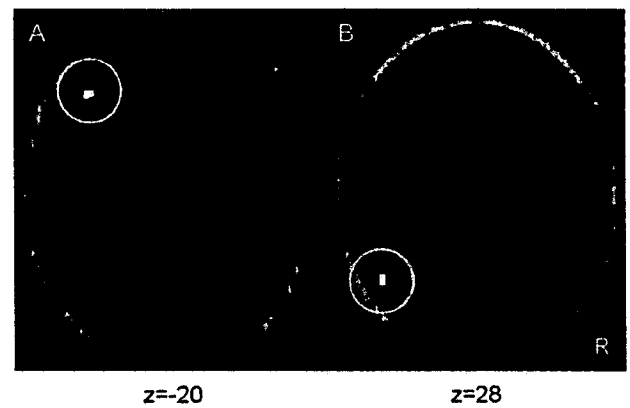

Figure 2. Correlations between self-ratings of (*A*) praiseworthiness (*B*) blameworthiness and brain activations. (*A*) Correlation between self-rating of praiseworthiness and degree of activation in left OFC in MB − N contrast. (*B*) Correlations between self-rating of blameworthiness and degree of activation in pSTS in MD − N contrast. Within the images, R indicates right. Numbers at bottom indicate coordinates of Montreal Neurological Institute brain.